CR-102723

NAS 8-21408

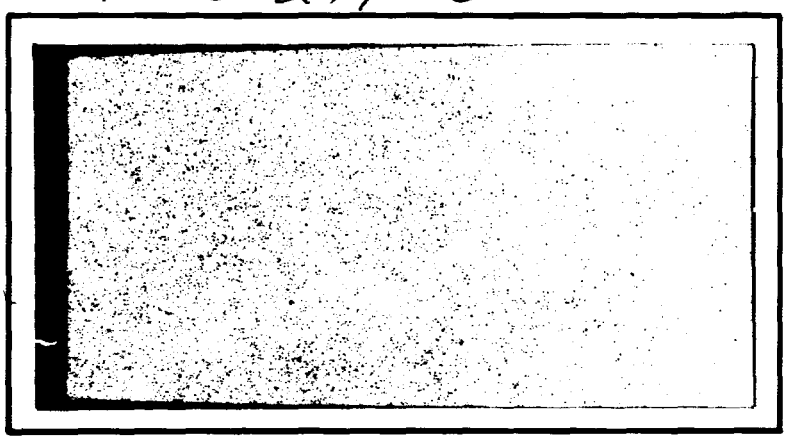

RYAN

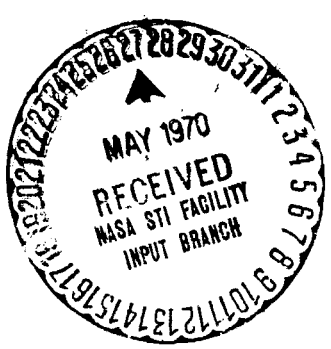

CR-102723

FINAL ENGINEERING REPORT

PHASED ARRAY
STEP RECOVERY DIODE MODULES

REPORT NO. 29167-6

MARCH 1970

PREPARED FOR

GEORGE C. MARSHALL SPACE FLIGHT CENTER

PREPARED BY

TELEDYNE RYAN AERONAUTICAL COMPANY

ELECTRONIC AND SPACE SYSTEMS

5650 KEARNY MESA ROAD

SAN DIEGO, CALIFORNIA 92112

TABLE OF CONTENTS

LIST OF ILLUSTRATIONS

SECTION 1
INTRODUCTION

Teledyne Ryan Electronic and Space Systems is investigating the applications of Step Recovery Diode (SRD) multipliers to control the phase of microwave phased array antenna systems. The program was supported by the Marshall Space Flight Center, Huntsville, Alabama, under Contract NAS 8-21408. This report describes the work performed under Modification No. 2, Exhibit "B" Section I - G and H.

The objective of this study was to improve the operation of an early model phased array transmitter described in Ryan Report No. 29163-30 dated 14 September 1967. The following tasks were performed:

1. Investigate improvement in transmitter efficiency by using transistors as power amplifiers following phase-controlled frequency multipliers, and phase stability of the amplifying and phase-controlling chain by closed loop techniques.

2. Construct, assemble and test an array of seven modules to demonstrate array behavior using transistor amplifiers.

   The demonstration array was designed and constructed for laboratory tests with no product engineering involved.

SECTION 2
SYSTEM DESCRIPTION

2.1 TRANSMITTER ARRAY DEFINITION

The phased array transmitter consists of seven microwave modules driven by a master oscillator-amplifier. Each module contains a phase controlled SRD frequency multiplier, an RF power amplifier and an antenna. Beam steering is accomplished by controlling the phase of the RF output of each module antenna. The output phase is controlled by changing the bias applied to the SRD frequency multiplier.

The seven modules are arranged in a linear array to form a fan shaped beam, narrow in azimuth and wide in elevation. Beam steering is in azimuth only since two axis steering had been previously demonstrated.

2.2 SYSTEM OPTIMIZATION

A preliminary study was conducted to determine the optimum method of obtaining higher power output per module. Three different methods were investigated for this application. The following methods were examined to determine maximum power output and cost.

1. A solid state oscillator operating at the output frequency and injection locked by an SRD multiplier.

2. An SRD frequency multiplier operating at the output frequency or a chain of SRD multipliers with one multiplier driving another multiplier.

3. An SRD frequency multiplier followed by one or more transistor amplifiers operating at the output frequency.

2.2.1 Injection Locked Oscillator

The block diagram of an injection locked oscillator is shown in Figure 1b. This method appeared to be the most efficient of the three methods considered. However, to obtain high efficiency several assumptions were necessary.

1. The phase error per module would be less than ± 10 degrees.

2. Load Q of the oscillator tuned circuits must be 150.

3. The free running frequency of the oscillator must be within 2.3 MHz of the SRD multiplier frequency.

These conditions were boundary values for -20 db locking ratio. That is conditions 1, 2, and 3 determined the point at which the oscillator would begin to become instable and tend to not phase lock.

If FM data bandwidths in excess of 1.15 MHz were required, the oscillator would become unlocked. This assumed that the oscillator had a free-running frequency exactly equal to the locking frequency. If the free-running frequency drifted, the FM data bandwidth would be reduced to (2.3-f)/2 MHz. This indicated that -10 db was a more reasonable locking level. At this level, the efficiency decreased to approximately 15%. At this lowered efficiency, the theoretical maximum FM data bandwidth would only be 12 MHz. A data bandwidth of 40 MHz was the design goal of the transmitter.

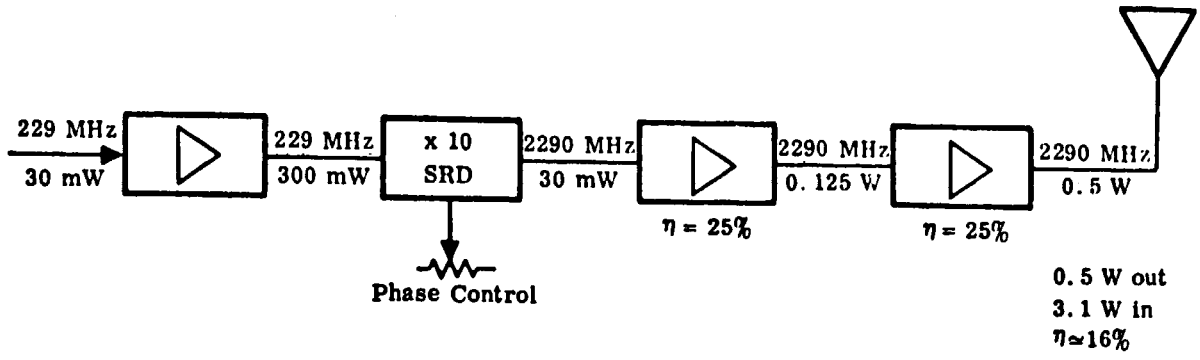

Figure 1a. Straight Transistor Amplifier

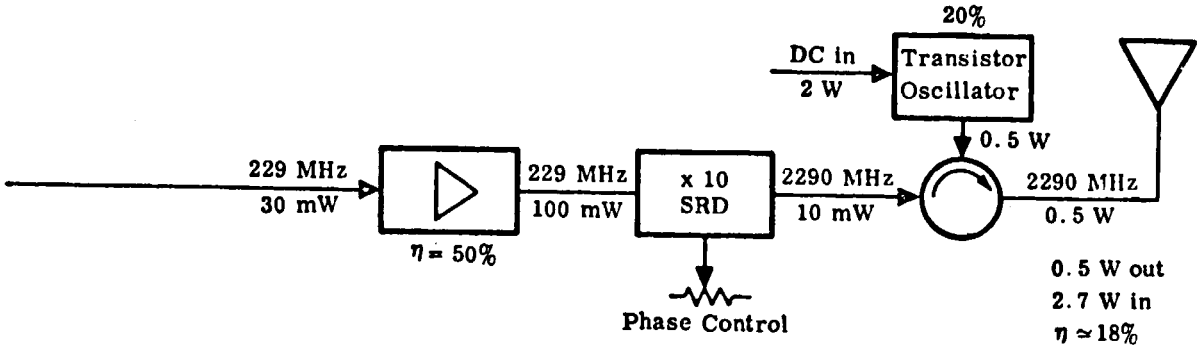

Figure 1b. Injection - Locked Oscillator

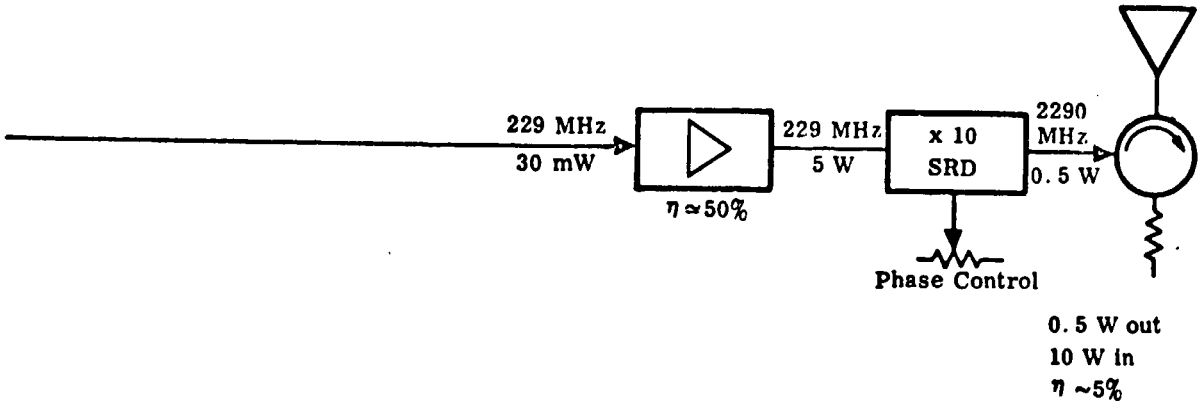

Figure 1c. Straight SRD Multiplier - Generator

2.2.2 SRD Frequency Multiplier

A block diagram of the power SRD multiplier is shown in Figure 1c. This is the "brute force" method of generating phase adjustable power at the output frequency and the method used on a previous transmitter. It provided more power output at 2.29 GHz than either of the other two methods at the time the study was conducted.

The generation of high power in the SRD multiplier leads to problems in thermal phase shift and power dissipation. This method also requires a high power driver amplifier which also has a heat dissipation and thermal drift problem. An efficiency of 10% in a X 10 SRD multiplier may be achieved if the thermal problems are not severe.

2.2.3 SRD Multiplier-Amplifier

A simplified block diagram of the SRD multiplier followed by a solid state amplifier is shown in Figure 1a. This method was selected to be a good compromise between complexity, reliability, efficiency and cost. The data bandwidth can be made as great as 1/N where N is the order of multiplication. The efficiency approaches that of a practical injection locked oscillator.

2.3 SYSTEM INVESTIGATIONS

2.3.1 Solid State Microwave Oscillators

Two solid state oscillators were constructed using different types of microwave transistors.

a. RCA TA 7403 - The RCA oscillator device is a coaxial package transistor utilizing the same "chip" as the RCA 2N5470. However, collector-base feedback capacity is deliberately introduced to insure the oscillator of the device. RCA claims 0.5 W output as a Colpitts oscillator at 2.0 GHz. At 2.29 GHz, the maximum power obtainable in our stripline circuit was 0.350 W. At this power output, the DC power input was 2.3 W (28 V at 120 MA). This is a calculated DC-RF efficiency of 15%. RCA claims 20% efficiency at 2.0 GHz. There are two reasons why the power and efficiency are lower than the data furnished by RCA. The first, and most obvious, is that the operating frequency of the transistor is above the specification point of 2.0 GHz. The second reason is that the device was intended to be used in a coaxial package. Using it in stripline necessitates several gross modifications of the geometry of the device.

b. Texas Instruments MS 0100 - The TI oscillator device is a stripline package device using beam-lead construction. TI claims 400 mw output at 2 GHz as a grounded-base oscillator. At 2.29 GHz the maximum power obtained was 300 mw. At this power output, the DC power input was 1.8 W (28 V at 65 MA) for a DC-RF efficiency of 22%. Again, the lower power and poor efficiency is the result of the higher frequency of operation.

2.3.2 Solid State Microwave Amplifiers

Three solid state amplifiers were constructed using three different transistors.

a. RCA 2N5470 - The RCA 2N5470 is the amplifier version of the TA 7403, less the internal feedback. It also is a coaxial package. RCA claims a power gain of 5 db at 2.0 GHz with a DC-RF efficiency of 30%. At 2.3 GHz, the power gain was 4.4 db (P_{in} = 200 mw P_o = 550 mw) and the DC input was 1.96 watts (28 volts at 70 MA), yielding a collector efficiency of 28%. The low power can be traced to the higher input frequency again.

b. TRW 2N5481 - Not much effort was expended in making an optimum design for the TRW device, in that the manufacturer's data sheet showed a rapid decay of characteristics above 2.0 GHz. A test of the device showed 410 mw out for 200 mw in (3.1 db) at 2.3 GHz, and a power input of 2.03 W (28 V at 75 MA) for a collector efficiency of 20%.

c. MSC 2001 - The MSC device is a stripline package amplifier characterized from 1.0 to 2.5 GHz. The manufacturer claims 6.0 db power gain at 2.3 GHz with a collector efficiency of 25%. At 2.3 GHz, our test showed 6.3 db gain (200 mw - 850 mw) with a power input of 3.15 watts (26.5 V at 118 MW) for a collector efficiency of 27%.

The operation of the devices tested is summarized in Table I.

Type	Power Out	RF Power In	DC Power In	Efficiency	Gain (db)
RCA					
TA 7403	350 mw	(osc)	2.3 W	15%	(osc)
2N 5470	550 mw	200 mw	1.96 W	28%	4.4
T.I.					
MS0100	300 mw	(osc)	1.8 W	22%	(osc)
TRW					
2N5481	410 mw	200 mw	2.03 W	20%	3.1
MSC					
MSC2001	850 mw	200 mw	3.15 W	27%	6.3

2.4 STUDY CONCLUSIONS

The results of the studies and experimental investigations indicated that the optimum transmitter configuration was a low power SRD frequency multiplier followed by a power amplifier chain.

SECTION 3

3.0 TRANSMITTER DESIGN

A block diagram of the SRD transmitter is shown in Figure 2. A crystal controlled oscillator generates the reference frequency of 114.5 MHz which is doubled to 229 MHz. The output of the doubler is passed through a power amplifier to produce an output of 10 watts at 229 MHz. A voltage controlled oscillator operating at 229 MHz may be substituted for the crystal controlled oscillator to provide a frequency modulated reference signal.

The output of the 229 MHz power amplifier is applied to a reactive power divider. This divides the drive power into seven isolated ports with 1.4 watts at each output. Each output of the power divider is connected to a transmitter module.

3.1 TRANSMITTER MODULE

The seven modules are identical and each consists of an SRD multiplier, Class A driver amplifier, Class C power amplifier and radiating element. A transmitter module is shown in Figure 3.

3.1.1 SRD Multiplier

The RF input to the module is 1.4 watts at 229 MHz. This power is applied to the input of an SRD frequency multiplier which multiplies the input by ten to an output frequency of 2290 MHz.

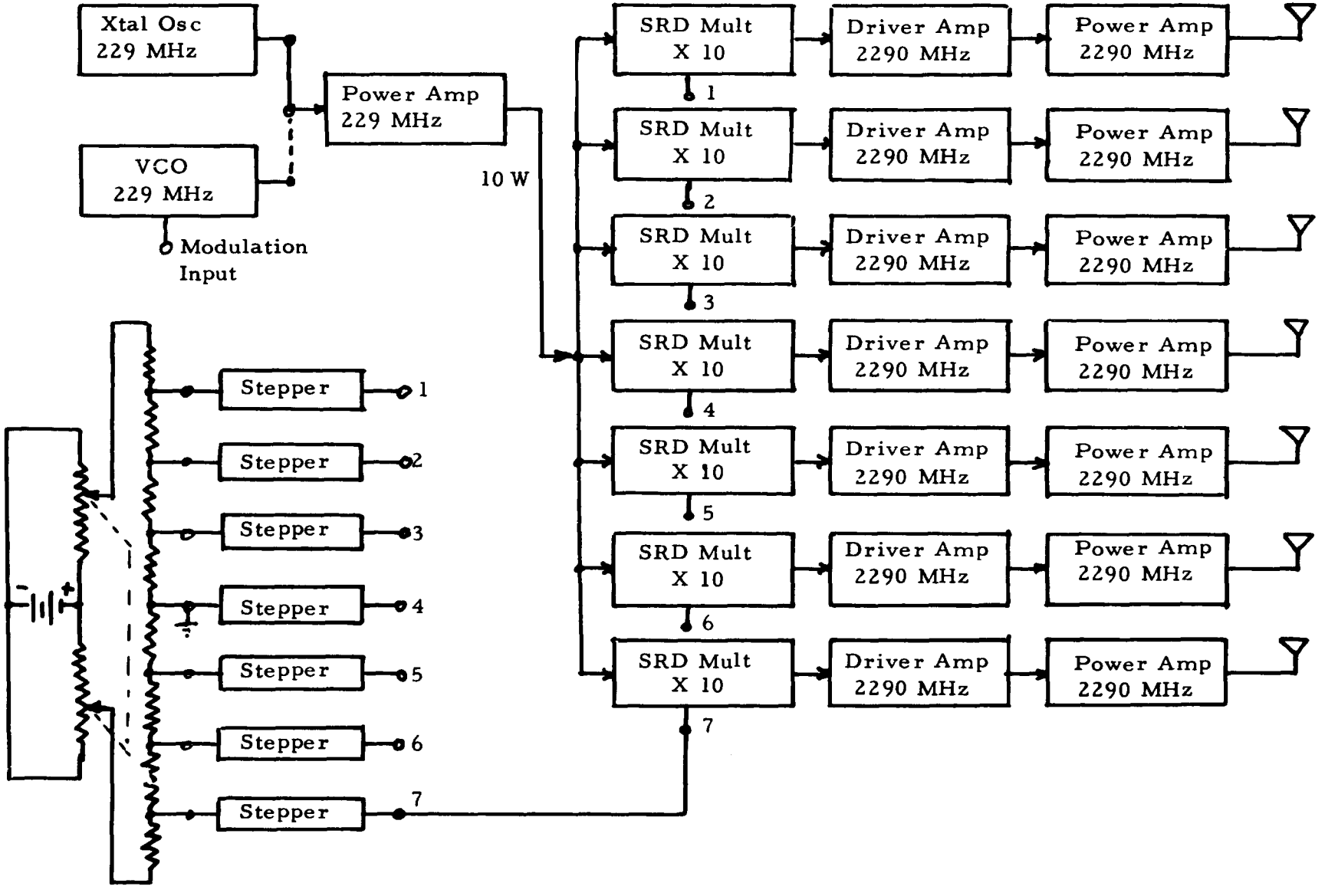

Figure 2. Transmitter Block Diagram

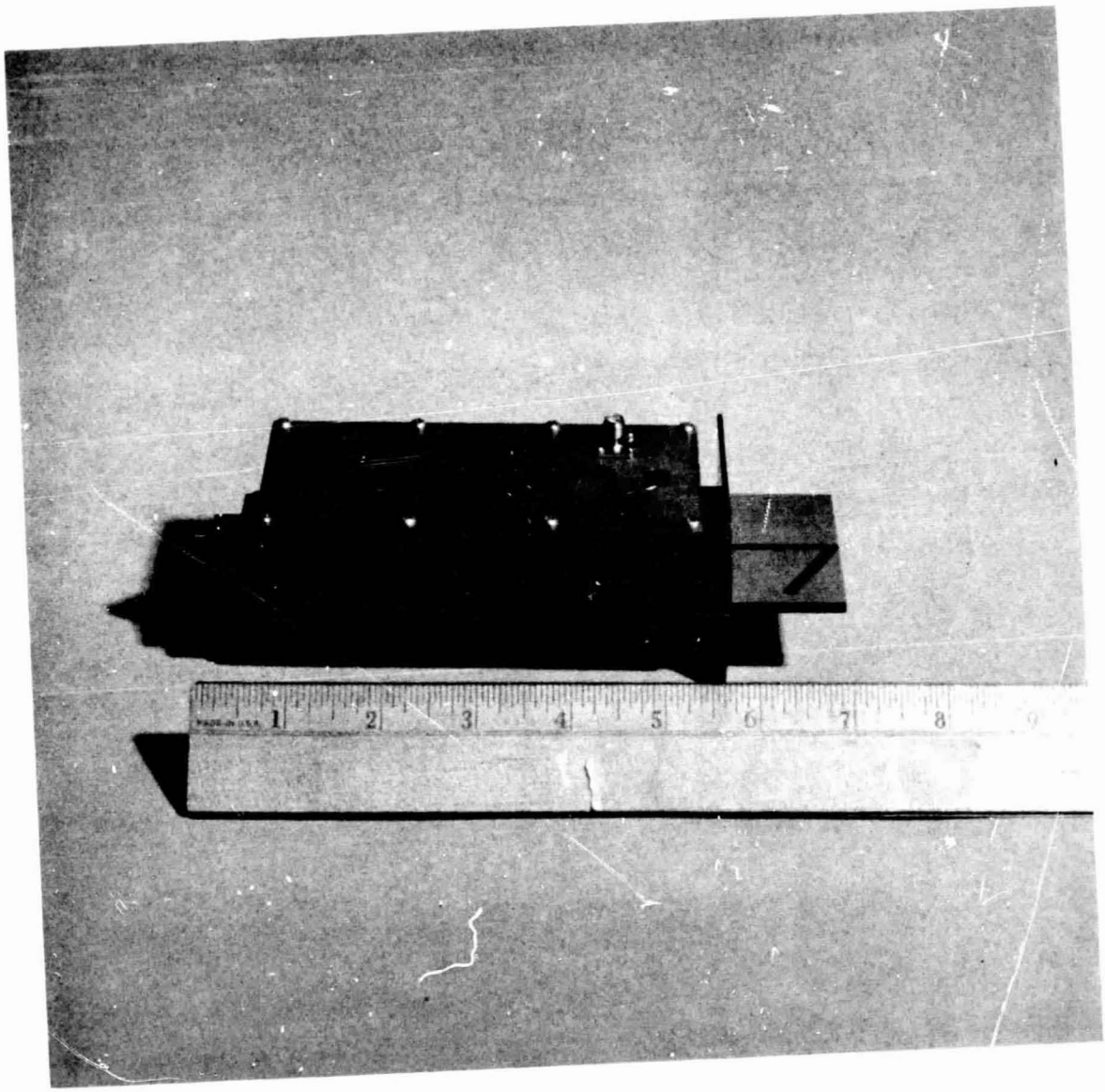

Figure 3. Transmitter Module

The step recovery diode has two discrete states of reactance and switches very rapidly between these two states. During the forward bias of the RF cycle, the impedance is very low and charge is stored near the junction in form of minority carriers. During the reverse cycle of RF, these minority carriers act to keep the SRD impedance low until all of the carriers have been swept out of the junction. At this point the diode steps or snaps to a high impedance state.

When the diode steps, a sharp transient is formed across the diode. This transient is allowed to ring down in an output resonator filter to produce the output which is ten times the input frequency.

The phase of the output of the SRD multiplier is controlled by changing the bias applied to the SRD. This changes the point on the input cycle at which the diode snaps and advances or delays the time of the sharp transient. Thus the time at which the output cycle starts is varied with respect to the input or driving frequency. The phase shift is a linear function of the bias voltage as shown in Figure 4. As the bias voltage varied from approximately -0.7 to +0.7 volts, the output phase shifted from +180° to -180° for a total phase shift of 360°. The power output of the multiplier decreased approximately 0.5 db at each end of the phase shift curve.

The SRD multiplier shown in Figure 5 is a microstrip circuit printed on a teflon-fiberglass substrate. The HPA 0300 SRD diode is connected in shunt across the output line which is capacitively coupled to the output resonator filter.

RECORDING CHARTS
GRAPHIC CONTROLS CORPORATION
BUFFALO, NEW YORK
PRINTED IN U.S.A.

No. XY 1001-SP1

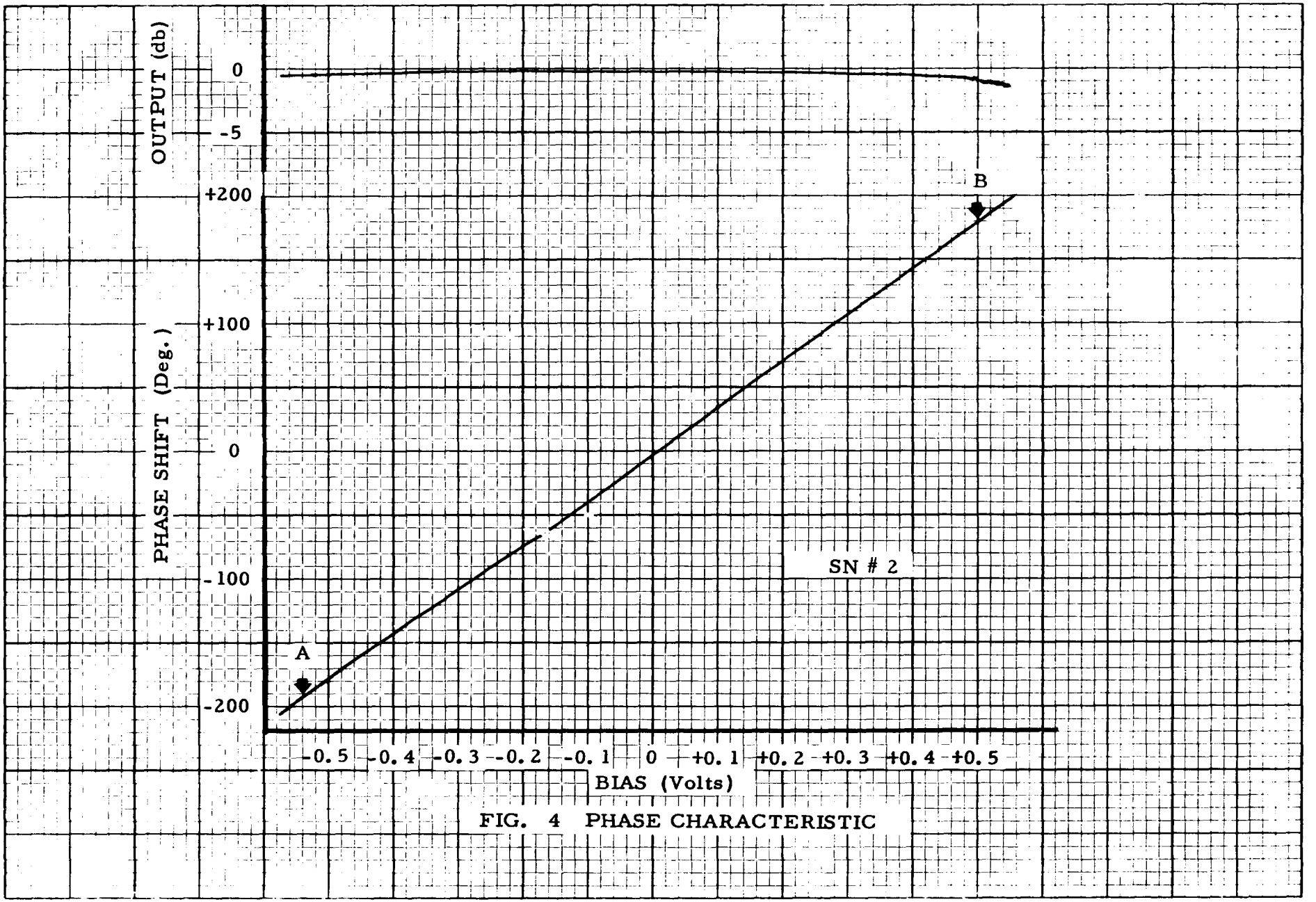

FIG. 4 PHASE CHARACTERISTIC

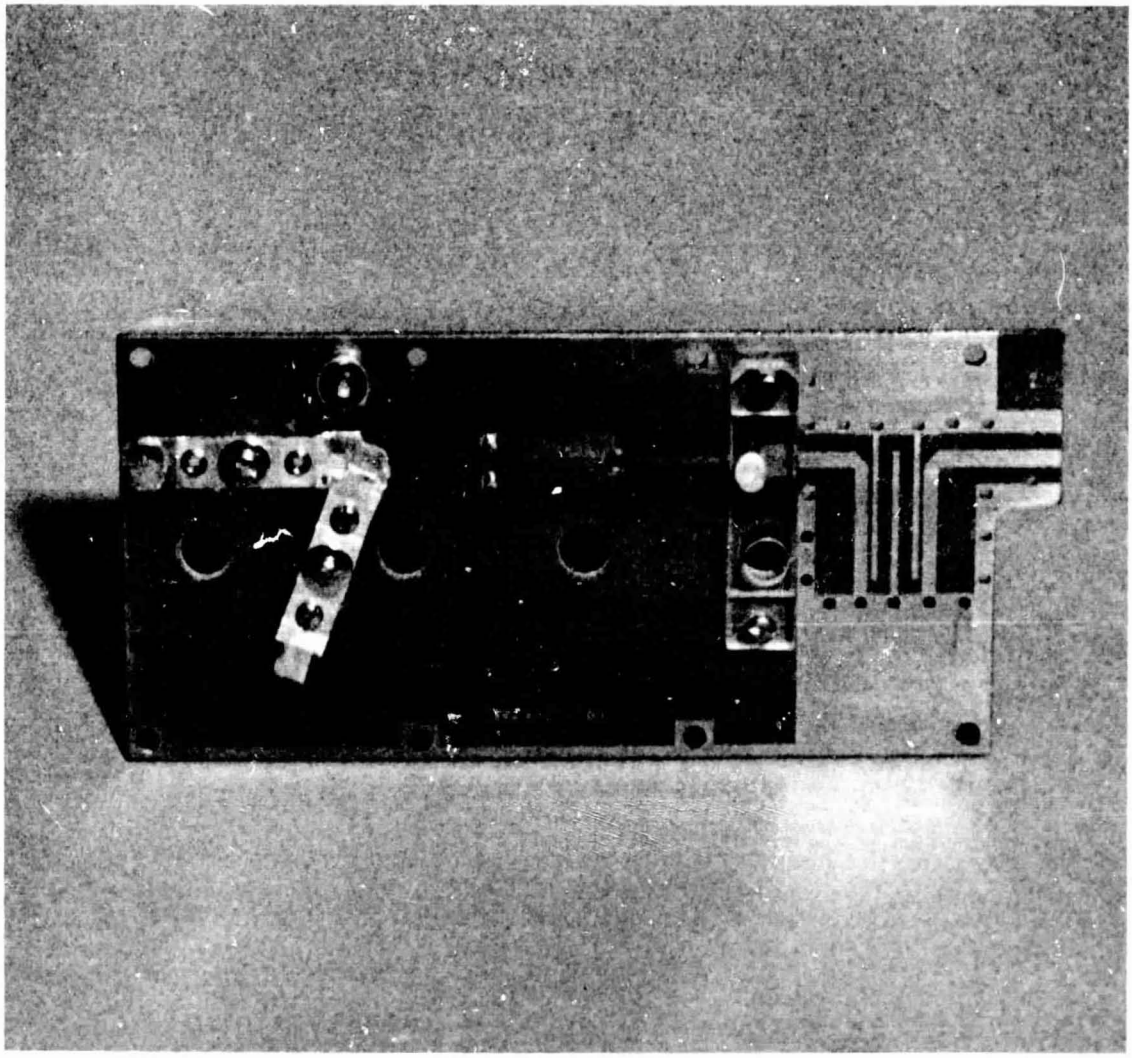

Figure 5. SRD Multiplier

The output filter is a stripline four pole, interdigital filter. The insertion loss is less than 0.5 db at the output frequency of 2290 MHz and the unwanted harmonics are suppressed by at least 30 db. The power output of the multiplier-filter is approximately 100 milliwatts.

3.1.2 Microwave Amplifier

The output of the multiplier is amplified by a two stage amplifier. Both stages are MSC 2001 microwave transistors manufactured by the Microwave Semiconductor Corporation. This transistor was designed to be driven at a power level of 200 mw for Class C operation at 2000 MHz. The first stage is operated Class A since the SRD multiplier output of 100 mw was too low to drive the first stage Class C. The output of the first stage is 225 milliwatts. This output is coupled through an impedance matching network to the input of the second stage. The network consists of two variable capacitors and a short section of transmission line.

The second stage is an MSC 2001 operating Class C. This stage produces an output of approximately 1.0 watt with an input of 225 milliwatts. The DC power input is 3.15 watts for a collector efficiency of 27%. Output of the second stage is coupled through a variable series capacitor and a short section of microstrip transmission line to the stripline antenna. No load isolator is used between the amplifier and the antenna. The microwave amplifier chain is shown in Figure 6.

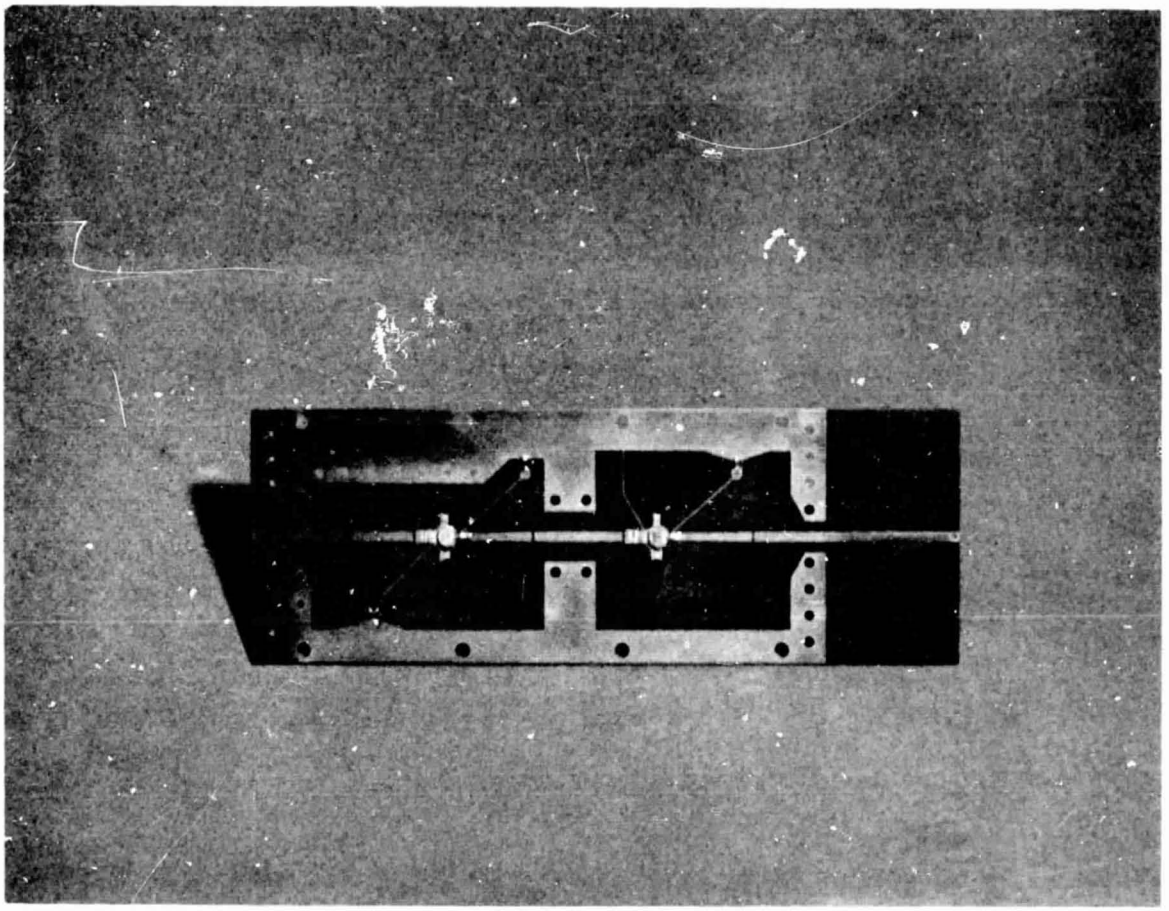

Figure 6. Microwave Amplifier Chain

3.1.3 Radiating Element

The radiating element is a printed circuit dipole center-fed by a stripline balun. The balun matches the 50 ohm unbalanced microstrip input to the balanced 72 ohm impedance at the center of the dipole. The arms of the dipole are swept back toward the ground plane to equalize the beamwidth of the E and H patterns. The beamwidth in each plane is approximately 110° at the 3.0 db points.

3.2 BEAM STEERING

In a linear array of n isotropic equally spaced elements, the phase between successive elements required to steer the antenna beam is:

$$\phi = \frac{2\pi d}{\lambda} \; n \sin \theta$$

d = element spacing

λ = operating wavelength

θ = angle between the beam maximum and the normal of the array axis

n = number of elements in the array

If the reference is in the center of the array, the phase becomes:

$$\phi = \frac{2\pi d}{\lambda} \left[(n-1) - \frac{(x-1)}{2} \right] \sin \theta \quad (n = 1, 2, 3 \ldots . x)$$

The phase shift required to steer the beam of a seven element linear array with the elements spaced one-half wavelength is shown in Table I. The bias voltages applied to the SRD multipliers to achieve these phase shifts are produced by a resistive voltage divider shown in Figure 2. Movement of the gauged potentiometers causes the voltage across the divider to increase or decrease in a positive or negative polarity. The fixed resistors divide the applied voltage into the proper values to cause the beam to scan.

The output of each junction of the divider is applied to a voltage stepping circuit which limits the phase shift of any module to 360 degrees. The phase shift curve of module # 2 is shown in Figure 4.

TABLE I

Scan Angle	Element Phase (Electrical Degrees) 1	2	3	4	5	6	7
0°	0	0	0	0	0	0	0
10°	-93	-62	-31	0	+31	+62	+93
20°	-183 +177	-122	-61	0	+61	+122	+183 -177
30°	-270 +90	-180 +180	-90	0	+90	+180 -180	+270 -90
40°	-348 +12	-232 +128	-116	0	+116	+232 -128	+348 -12
50°	-414 -54	-276 +84	-138	0	+138	+276 -84	+414 +54
60°	-468 -108	-312 +48	-156	0	+156	+312 -48	+468 +108
70°	-510 -150	-340 +20	-170	0	+170	+340 -20	+510 +150
80°	-531 -171	-354 +6	-177	0	+177	+354 -6	+531 +171
90°	-540 -180	-360 0	-180 +180	0	+180 -180	+360 0	+540 +180

Assume that at boresight (Az = 0) the voltage on # 2 is zero volts. As the scan control is moved in the direction to cause the bias of # 2 to become more negative, the phase will continue to shift until a bias of -0.54 volts is reached at point A. At this point the phase of # 2 has shifted -180° which would produce a scan of 30° from boresight as shown in Table I. If the steering control is moved more negative, the "stepper" produces a sudden step in the bias voltage to point B. This shifts the phase of # 2 by a 360° step to +180° which is the same as -180° phase. Thus the stepper circuit steps the steering control voltage so that each SRD multiplier shifts phase over the most linear 360° portion of its characteristic.

3.2.1 Phase Stepping Circuit

The basic circuit of the steering control is shown in Figure 7. A variable voltage from the voltage divider is applied to the input of the individual stepper unit. This voltage is applied to both the input operational amplifier and the sensing input of the Schmitt triggers. Assume that the input voltage has an initial value between O and V where O = 0° and V = 360° when applied to the SRD multiplier. When the input voltage is below V, the triggers do not operate and the amplified voltage appears at the output. If the input increases to V, the first trigger fires and places a step -V on the summing junction. This steps the output voltage back to O. When the input continues to increase to 2V, the second trigger fires and places an additional -V in parallel with the first step of -V thus removing 2V from the output. This series continues until (N+1) 360° steps have been traversed. N is the number of trigger units in the steering control.

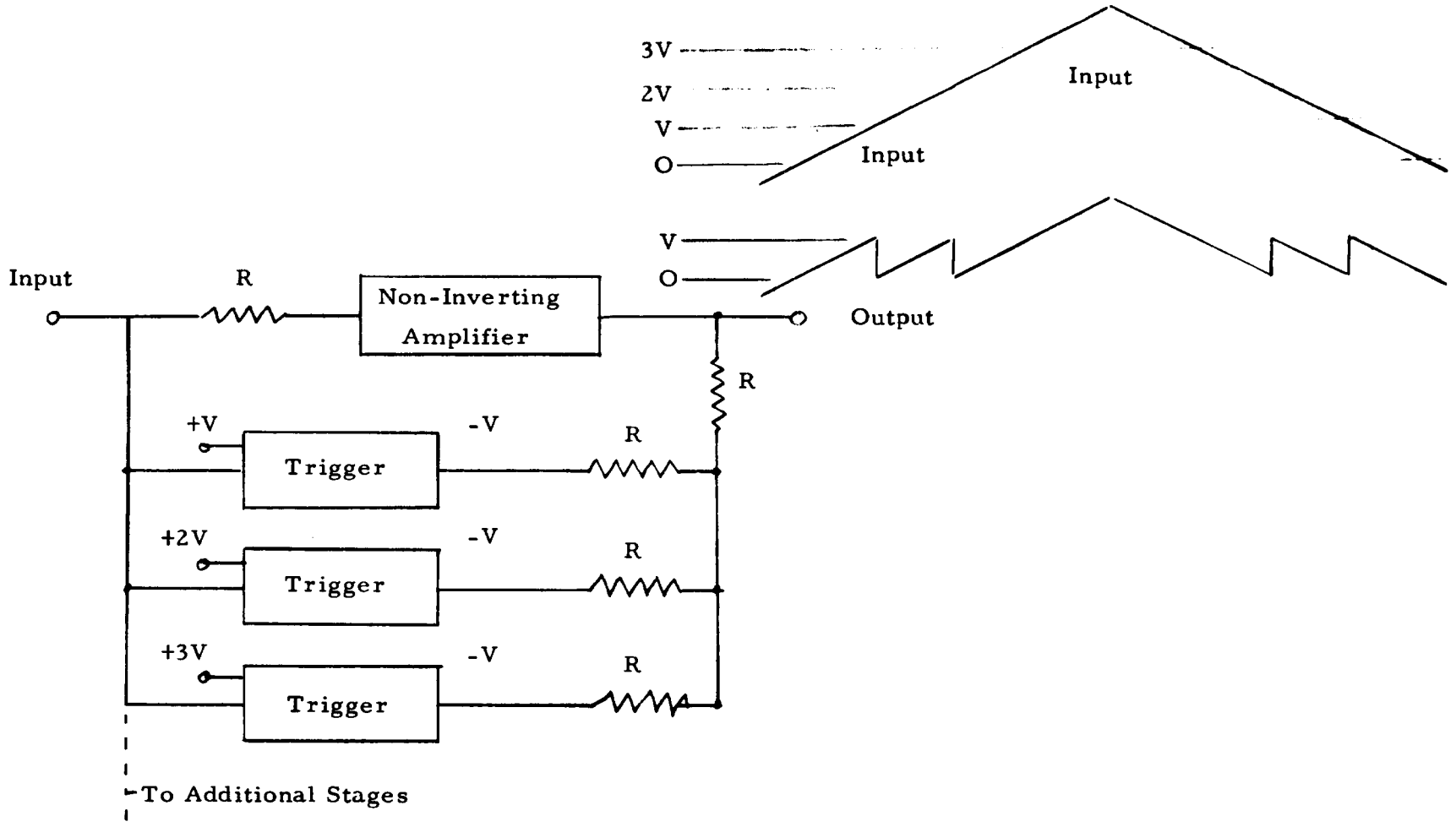

Figure 7. Stepping Circuit Block Diagram

A complete circuit diagram of a stepper circuit is shown in Figure 8. This is a three step circuit which will operate at speeds in excess of 1.0 KHz. A stepper is provided for each transmitter module although the center elements do not phase step. The stepper also contains the bias amplifiers, bias slope controls and a boresight phase adjustment. Each stepper circuit is mounted on a plug-in printed circuit board shown in Figure 9.

3.3 TRANSMITTER ARRAY ASSEMBLY

The experimental array consists of the seven transmitter modules mounted on a common aluminum heat sink in an aluminum housing. The antennas are spaced one-half wavelength on centers. This housing also contains the master oscillator, power amplifier and power divider. The array assembly shown in Figure 10 is 19" w x 7" h x 20" deep.

The power supplies and steering control circuits are mounted on a separate chassis shown in Figure 11. A single multiturn dial controls the azimuth position of the array beam. This position or scan angle is indicated by a zero center meter.

The plug-in steering logic cards are mounted back of the panel on the left side of the chassis. A single cable connects between the control unit and the array assembly. The control panel is a standard 19" x 7" panel and the chassis is 20" deep.

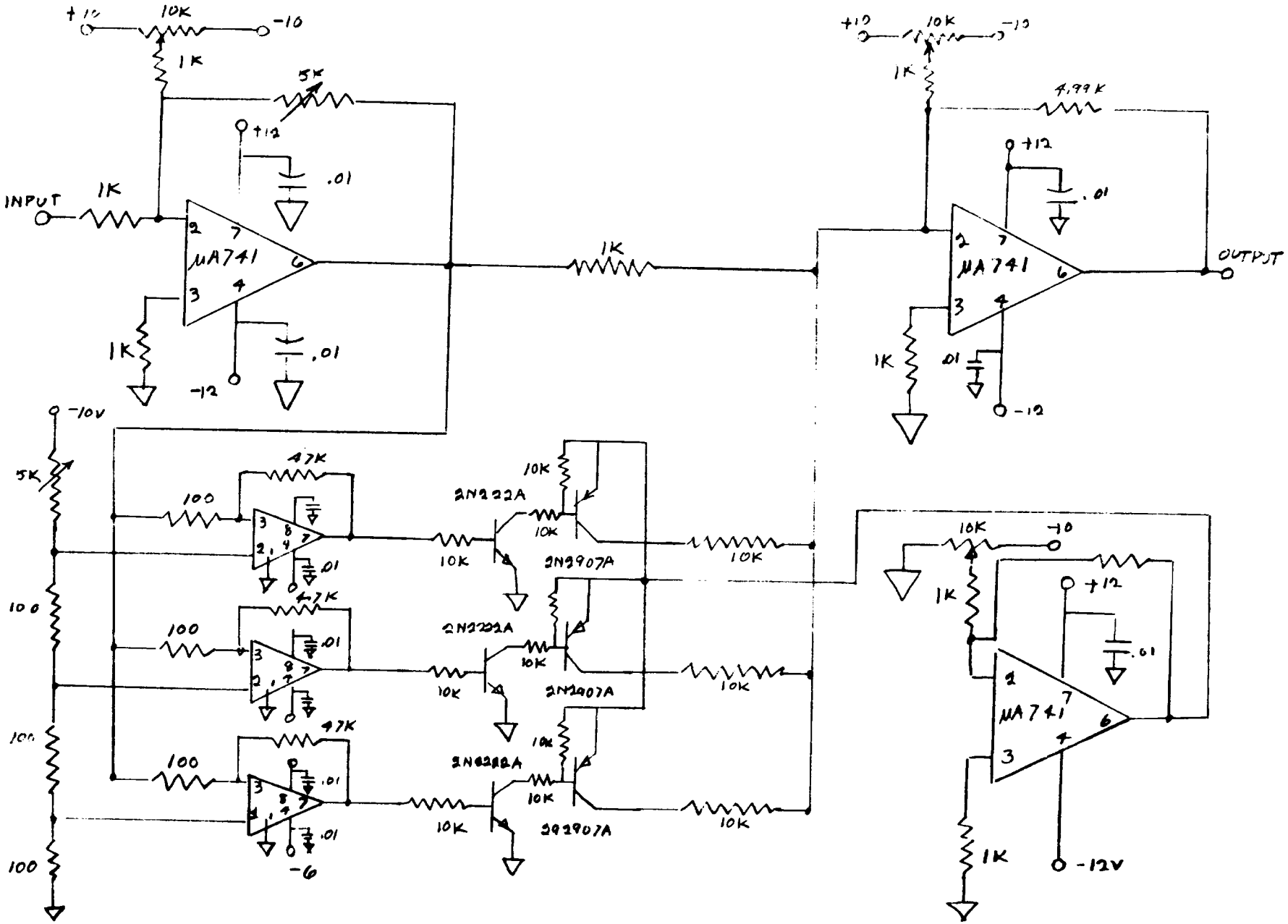

Figure 8. Stepper Circuit Diagram

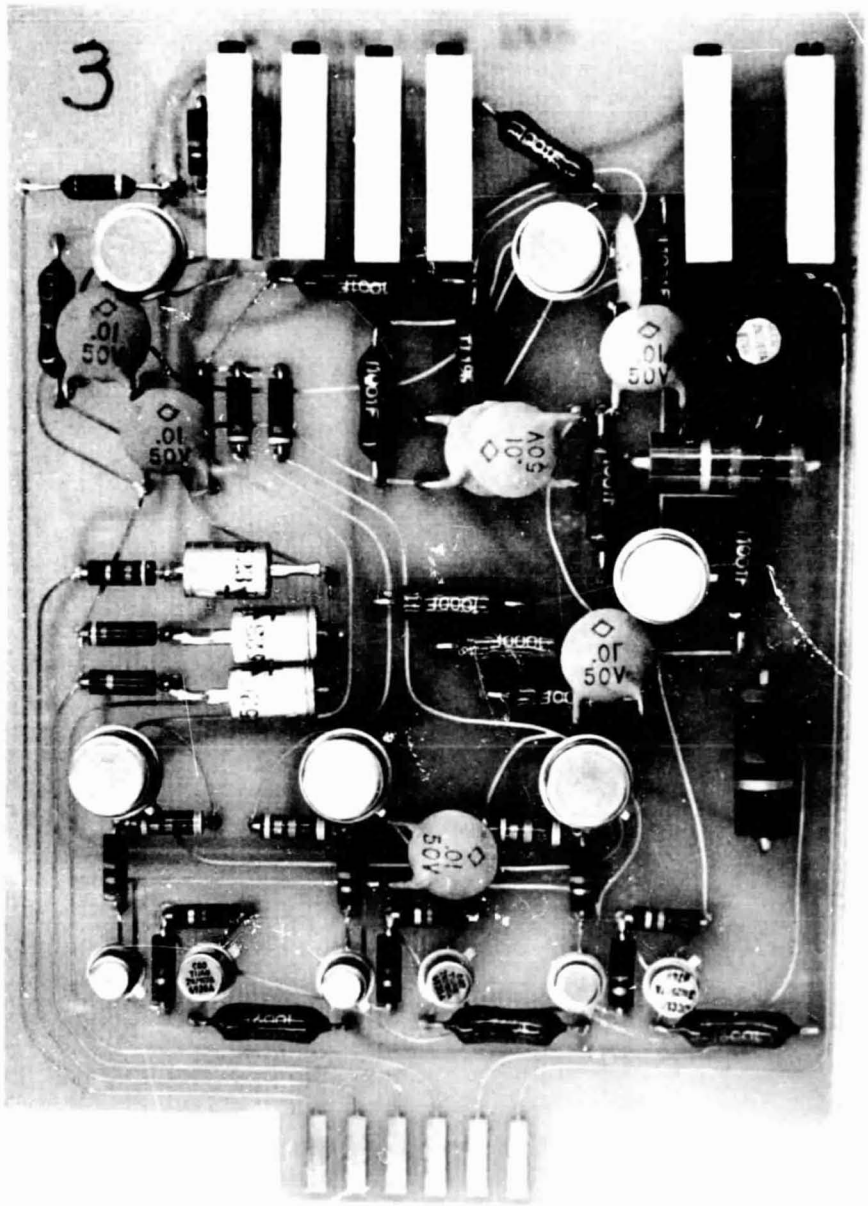

Figure 9. Stepper Circuit (Mounted on Plug-in Printed Circuit Boards)

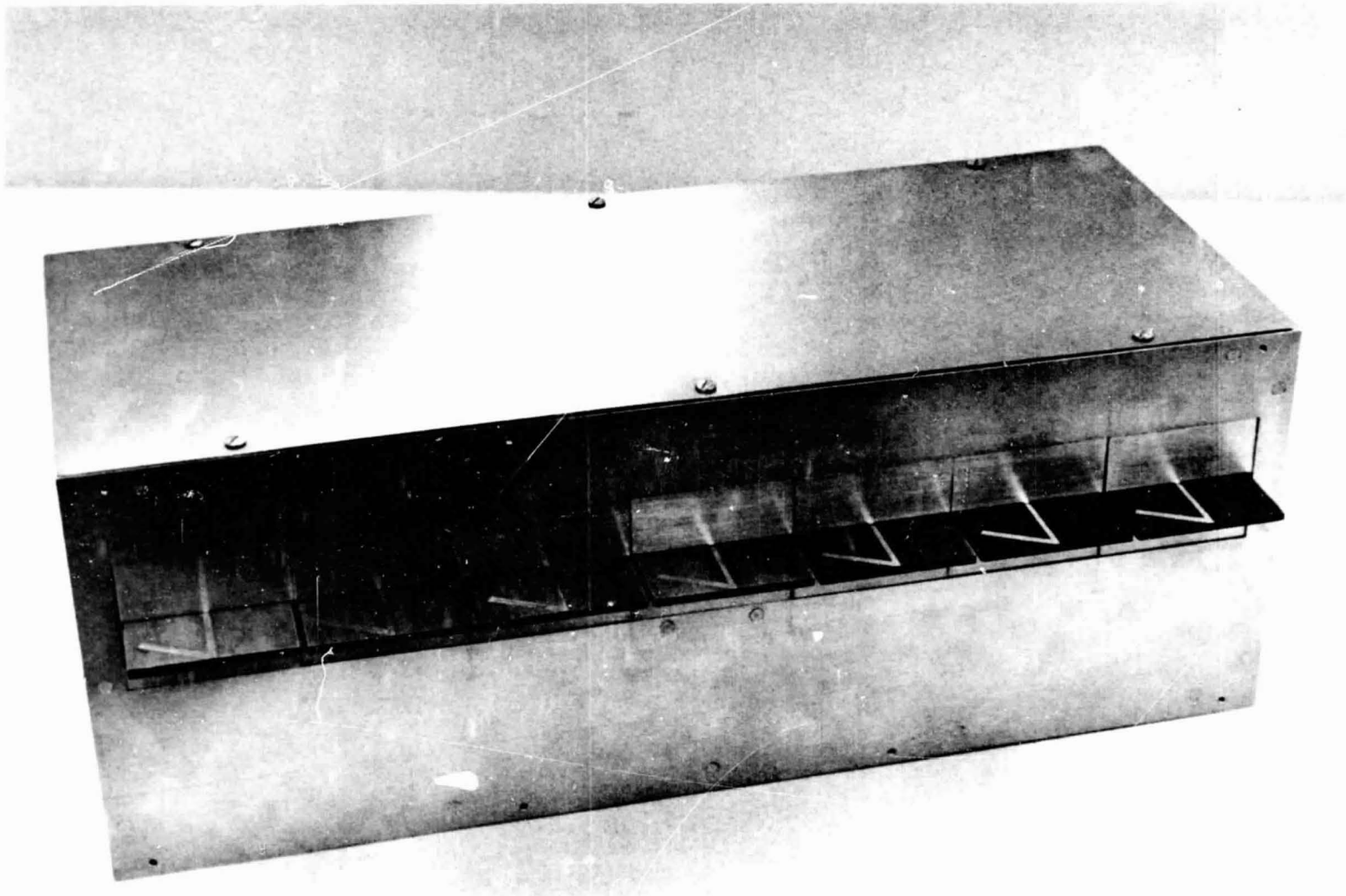

Figure 10. Array Assembly

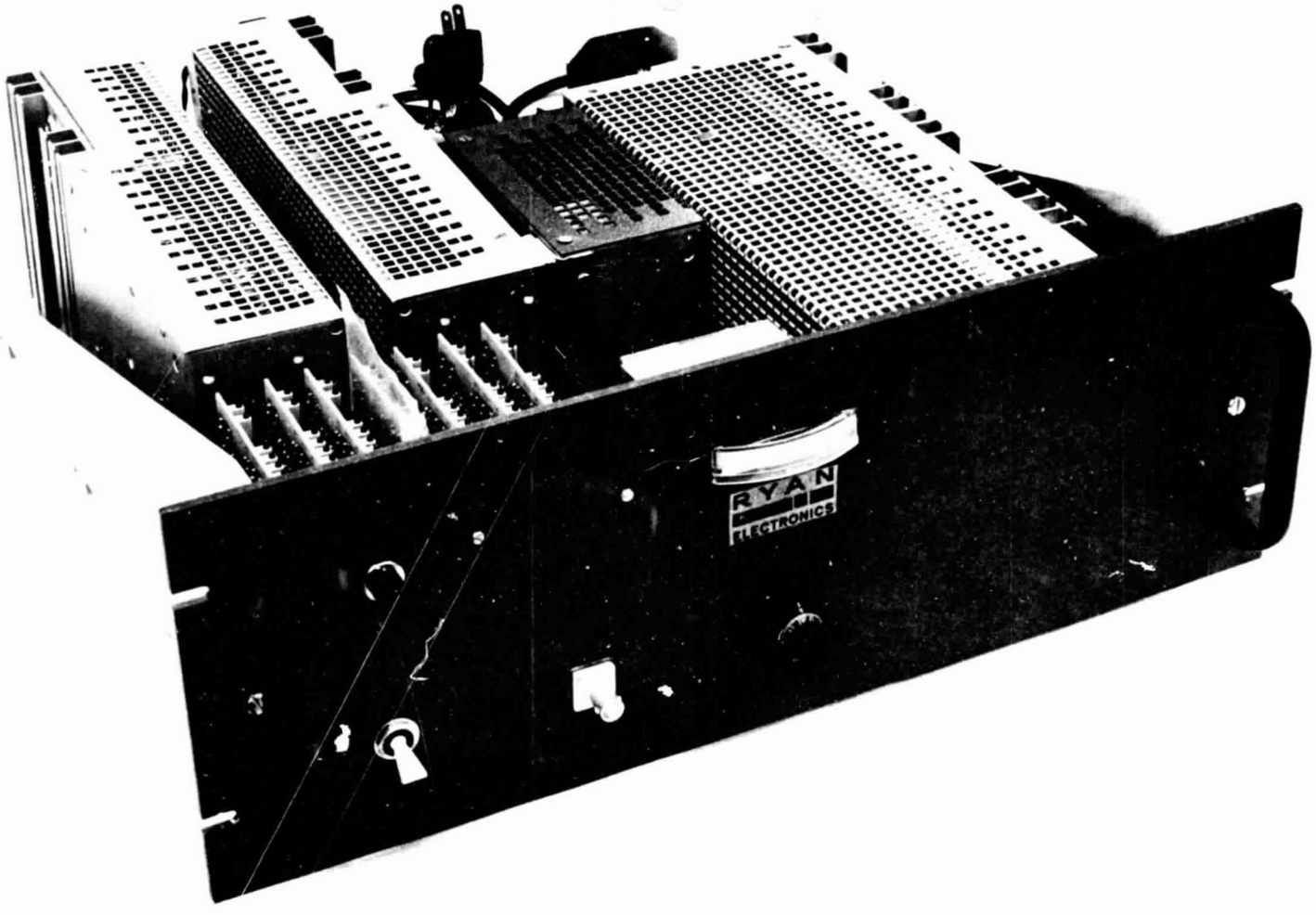

Figure 11. Power Supplies and Steering Control Circuits

SECTION 4

4.0 ARRAY TESTS

4.1 ANTENNA MUTUAL COUPLING

A number of tests were conducted to determine the amount of power radiated by one module and fed back into other modules in the array. This power fed into other modules through the mutual coupling of the antennas, disturbs the output impedance match of the module and usually produces erratic operation of the module.

This interaction due to mutual coupling may be minimized by ferrite load isolators in the antenna feed lines. These isolators maintain a one-way flow of power. Any reversed power is absorbed in a load and not passed back to the output device. The isolators are usually rather large, expensive and dissipate some forward power due to their insertion loss.

The mutual coupling tests were performed on the experimental array by placing an antenna removed from one of the modules in place of one of the modules in the array. The remaining modules were energized and the power fed into the test antenna measured. These tests showed that only a few milliwatts were fed into the test antenna. This indicated that the output impedance of the modules would not be disturbed and the load isolators could be omitted.

4.2 BEAM STEERING TESTS

The transmitting array was mounted on an antenna positioner as shown in Figure 12. The positioner was mounted on a wooden platform approximately 20 feet above the ground. The receiver was mounted in a wooden tower located 90 feet from the transmitter and 20 feet above the ground.

The array was set at boresight (Az = 0°) with all module outputs equal in phase and amplitude. The boresight E-plane pattern cut in azimuth is shown in pattern No. 1.* The beam shape was very good with a beamwidth of 14° at the half-power points (-3.0 db) which agrees with the calculated beamwidth of 14.5°. The first sidelobes were below the 13.5 db level calculated for a uniform linear array.

The steering dial was then rotated to produce scan angles of ±60 degrees. Patterns taken every 10 degrees are shown in Nos. 2 through 13. The antenna patterns on one side of boresight (arbitrarily designated negative) were very close to calculated patterns at the various scan angles. The gain at -60° scan was less than 3.0 db below the broadside gain. Beamwidths of the patterns increased as the scan angle increased due to the decrease of the effective aperture.

As the beam was scanned on the other (positive) side of boresight, the gain was slightly erratic with scan angle and the patterns did not agree as well with the theoretical patterns. The nulls were not as sharp on the positive side of boresight. The patterns show some phase and amplitude errors as the beam scanned.

* See Appendix for antenna patterns.

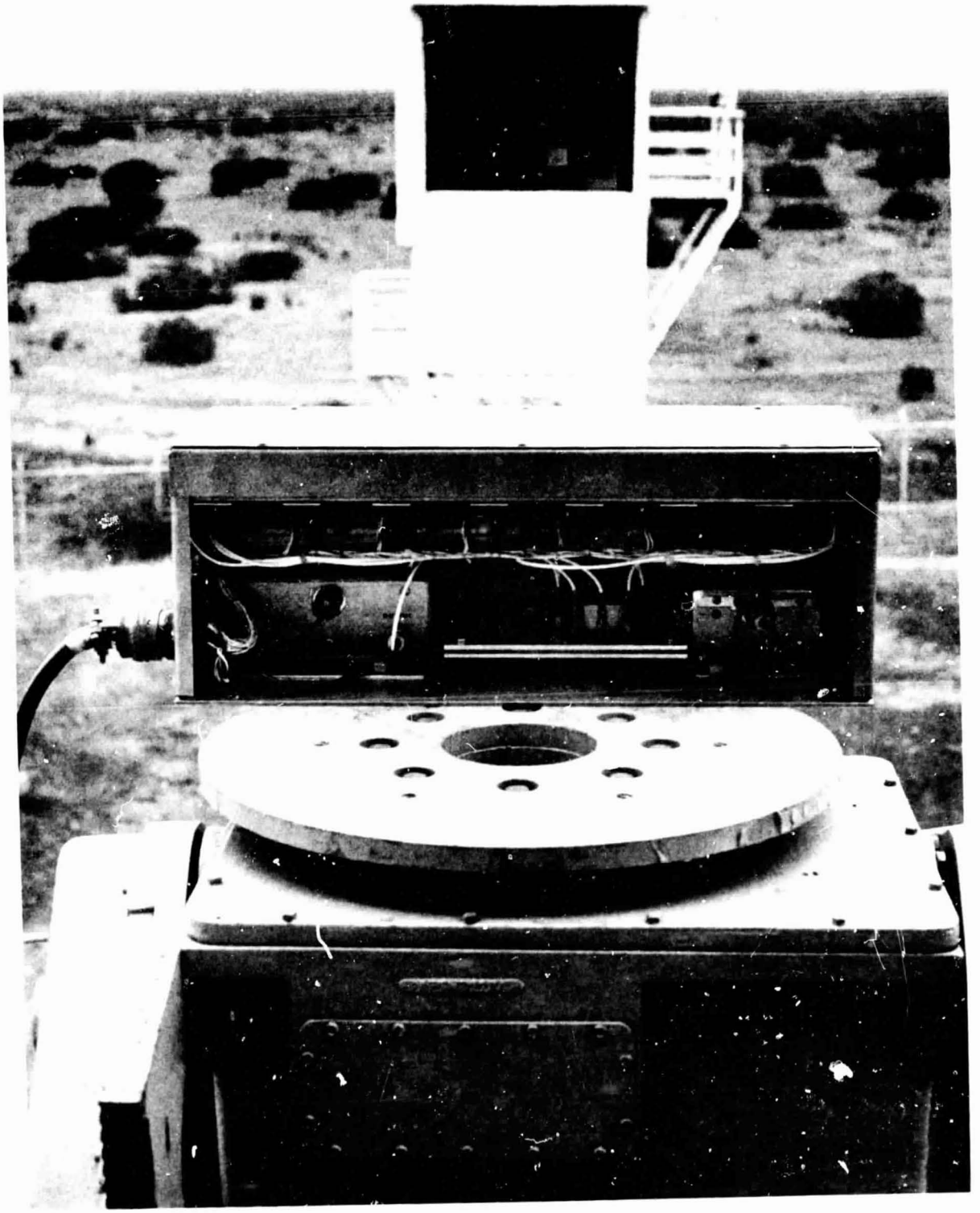

Figure 12. Beam Steering Test Setup

A number of patterns were run on the individual elements with the other elements operating. This was accomplished by driving the amplifier section of each individual module with an amplitude modulated signal while the other modules were operated unmodulated. Thus the pattern recorder received only the pattern of the modulated element.

These tests showed that the patterns of the individual elements were being distorted as the phase of the other elements was shifted to produce the scan. The effect of mutual coupling and interaction between the antennas was variable with scan and distorted the element patterns at some scan angles.

The interaction could be reduced by introducing metal baffles or shields between the dipoles as shown in Figure 13. This arrangement produced better patterns at scan angles up to ±30°. At larger scan angles the gain decreased rapidly due to the shadowing of the shield which restricted the element pattern in azimuth angle.

Additional tests were conducted to determine the effects of frequency modulating the master oscillator of the array. A voltage controlled oscillator was substituted for the crystal controlled oscillator and various modulation frequencies applied to the VCO. The patterns with modulation were very similar to those obtained in the CW condition. However, the VCO was not very stable with temperature and the good patterns became distorted as the VCO drifted over long periods of time.

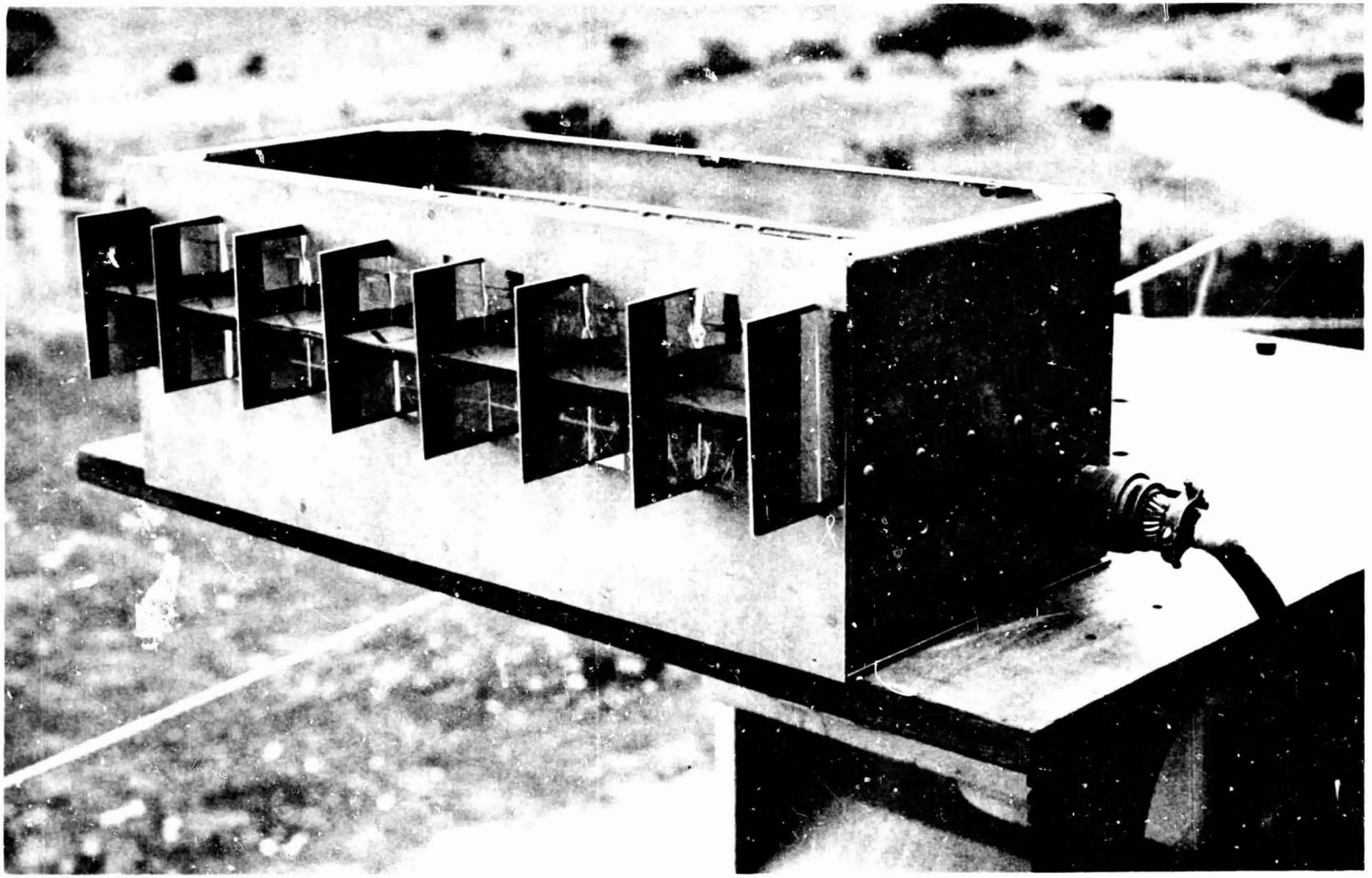

Figure 13. Transmitting Array with Baffles Installed Between Dipoles

A further test was conducted by modulating the transmitter array with the data from a high resolution, 1000 line television camera. The picture was received by a thirty-six element SRD phased array receiver. The transmitter beam was electronically steered toward a reflector on the pattern range and the receiver was steering to receive the reflected transmitter beam. Good quality TV pictures were received at various scan angles of both transmitter and receiver.

4.3 SUMMARY AND CONCLUSIONS

The primary objective of this study was to improve the efficiency of the SRD phase controlled transmitter using state of the art components. The original coaxial transmitter module delivered 100 milliwatts to each antenna. It was 2.5 x 2.5 x 37.5 inches and weighed more than four pounds. The stripline module developed in this study delivers 1.0 watt to the antenna. This module is 2.5 x 2.5 x 7 inches and weighs less than a pound. The beam steering circuit was greatly simplified and is capable of high speed scan.

The study has demonstrated that a phased array transmitter using an SRD phase controlled frequency multiplier followed by a transistor amplifier has the following advantages.

1. The array beam may be scanned continuously and rapidly through wide angles by means of a very simple analog device.

2. Beam steering is accomplished by a very efficient method since it combines the phase shift function with a solid state

frequency multiplier. The frequency multiplier is required in most coherent microwave systems.

The transistors used in the amplifier chain were early models of a new series of transistors. Later transistors are capable of producing outputs greater than 1.0 watt. Much higher output per module may be obtained by operating these transistors in parallel combinations.

The pattern tests show that the interactions between the transmitter modules disturbed the output of the transistor amplifiers as the beam was scanned. This interaction may be eliminated by inserting ferrite load isolators between the output of the amplifiers and the antennas.

The transmitter modules may be further reduced in size and weight by using microcircuit instead of stripline design. The MIC design uses a higher dielectric constant substrate such as alumina or sapphire. This reduces the size of the circuits and eliminates the cover board.

APPENDIX

ANTENNA PATTERNS

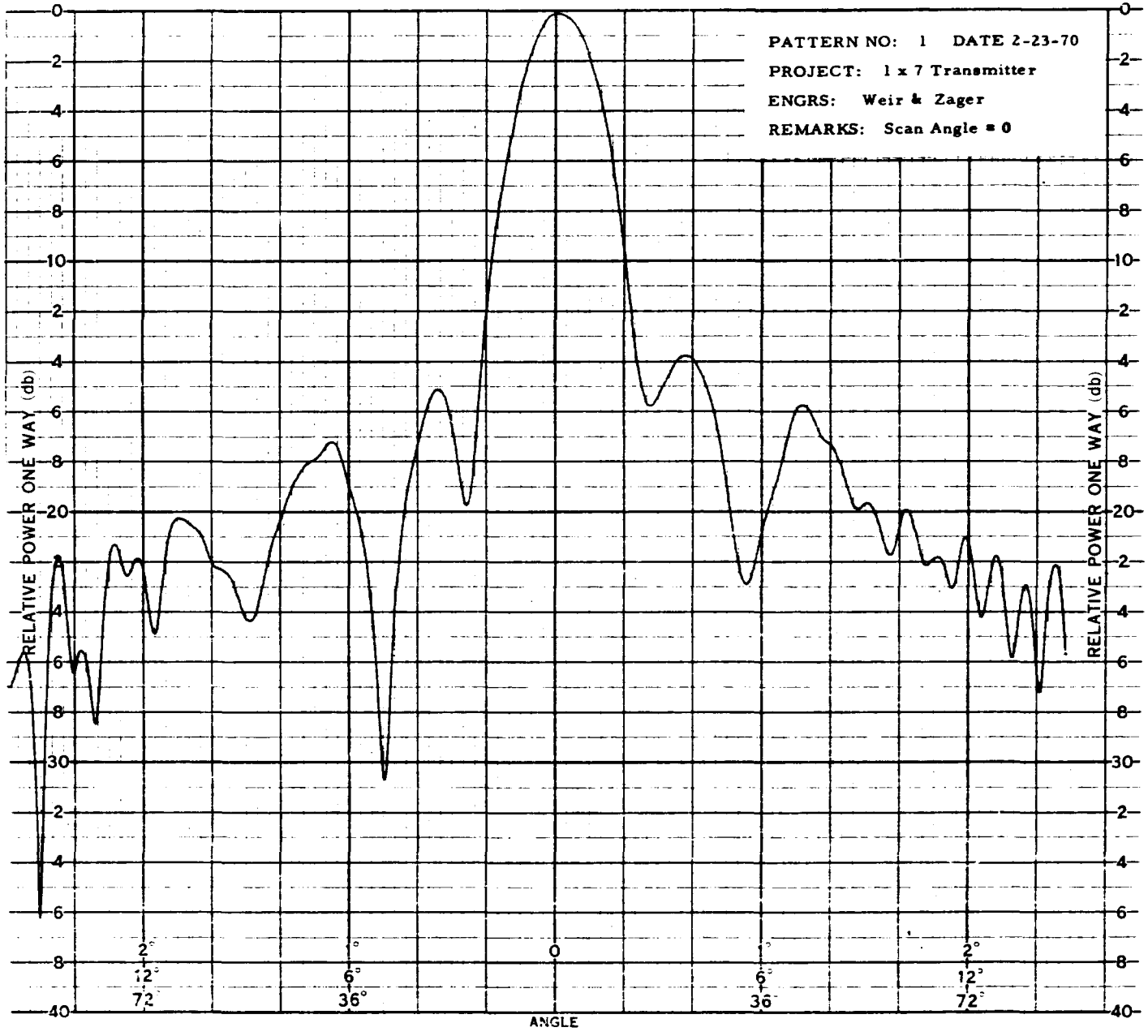
PATTERN NO: 1 DATE 2-23-70
PROJECT: 1 x 7 Transmitter
ENGRS: Weir & Zager
REMARKS: Scan Angle = 0
RELATIVE POWER ONE WAY (db)
RELATIVE POWER ONE WAY (db)
0
2
4
6
8
10
20
30
40
2°
12°
72°
6°
36°
0
6°
36°
2°
12°
72°
ANGLE

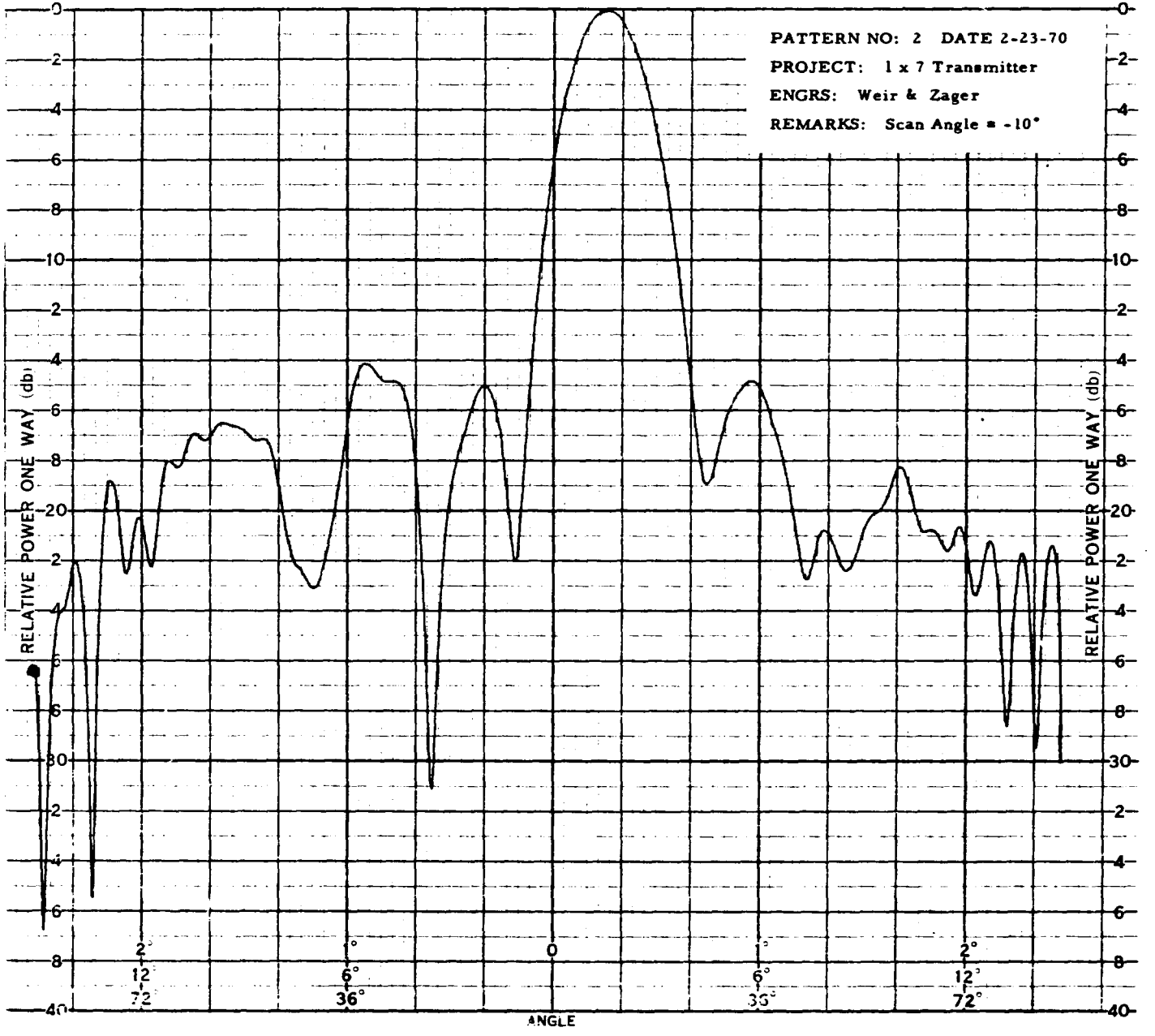
PATTERN NO: 2 DATE 2-23-70
PROJECT: 1 x 7 Transmitter
ENGRS: Weir & Zager
REMARKS: Scan Angle = -10°
RELATIVE POWER ONE WAY (db)
RELATIVE POWER ONE WAY (db)
0
2
4
6
8
10
20
30
40
2°
12
72
1°
6°
36°
0
1°
6°
36°
2°
12°
72°
ANGLE

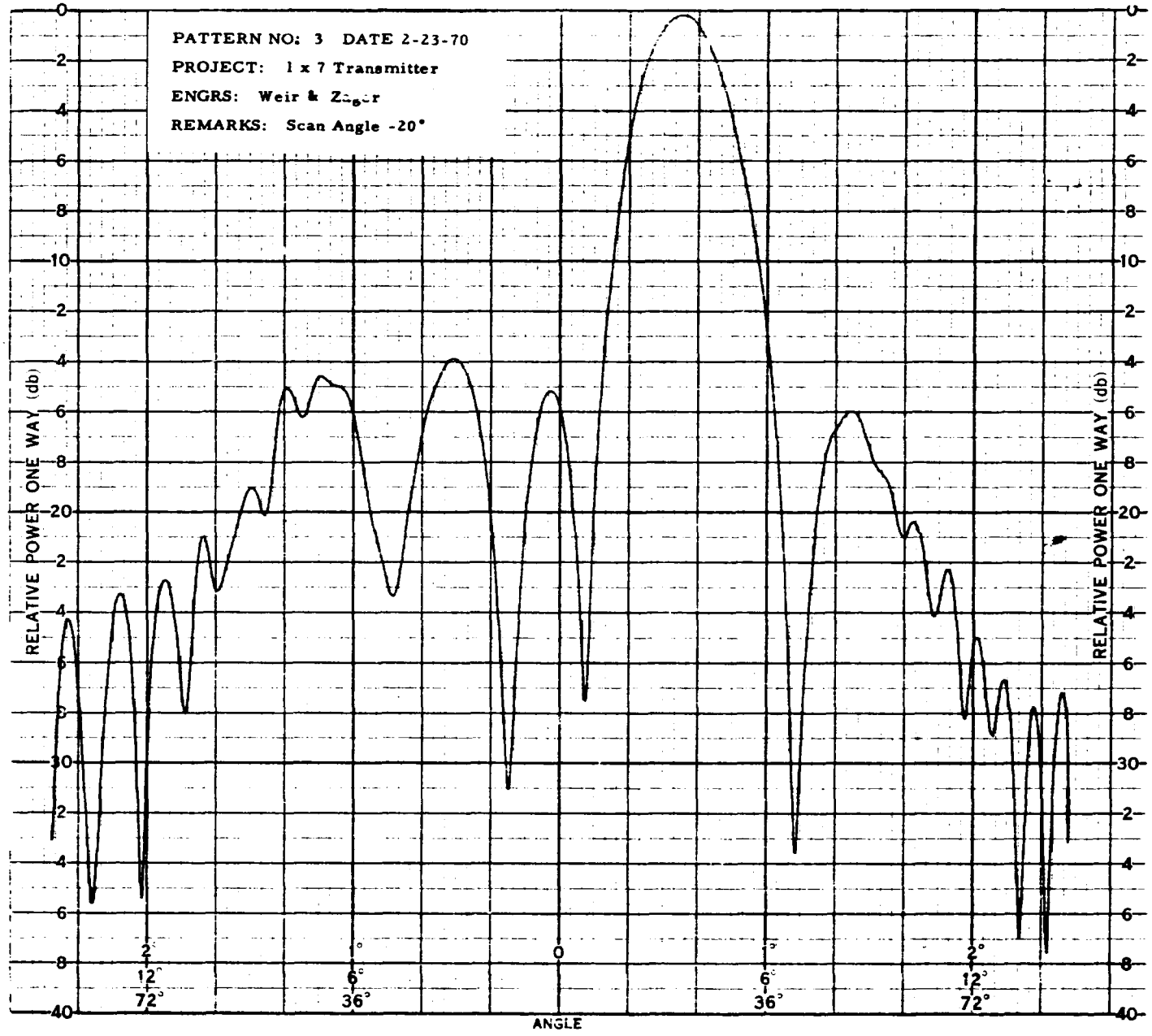
PATTERN NO: 3 DATE 2-23-70
PROJECT: 1 x 7 Transmitter
ENGRS: Weir & Zaeger
REMARKS: Scan Angle -20°
RELATIVE POWER ONE WAY (db)
RELATIVE POWER ONE WAY (db)
0
2
4
6
8
10
20
30
40
2°
12°
72°
6°
36°
0
6°
36°
2°
12°
72°
ANGLE

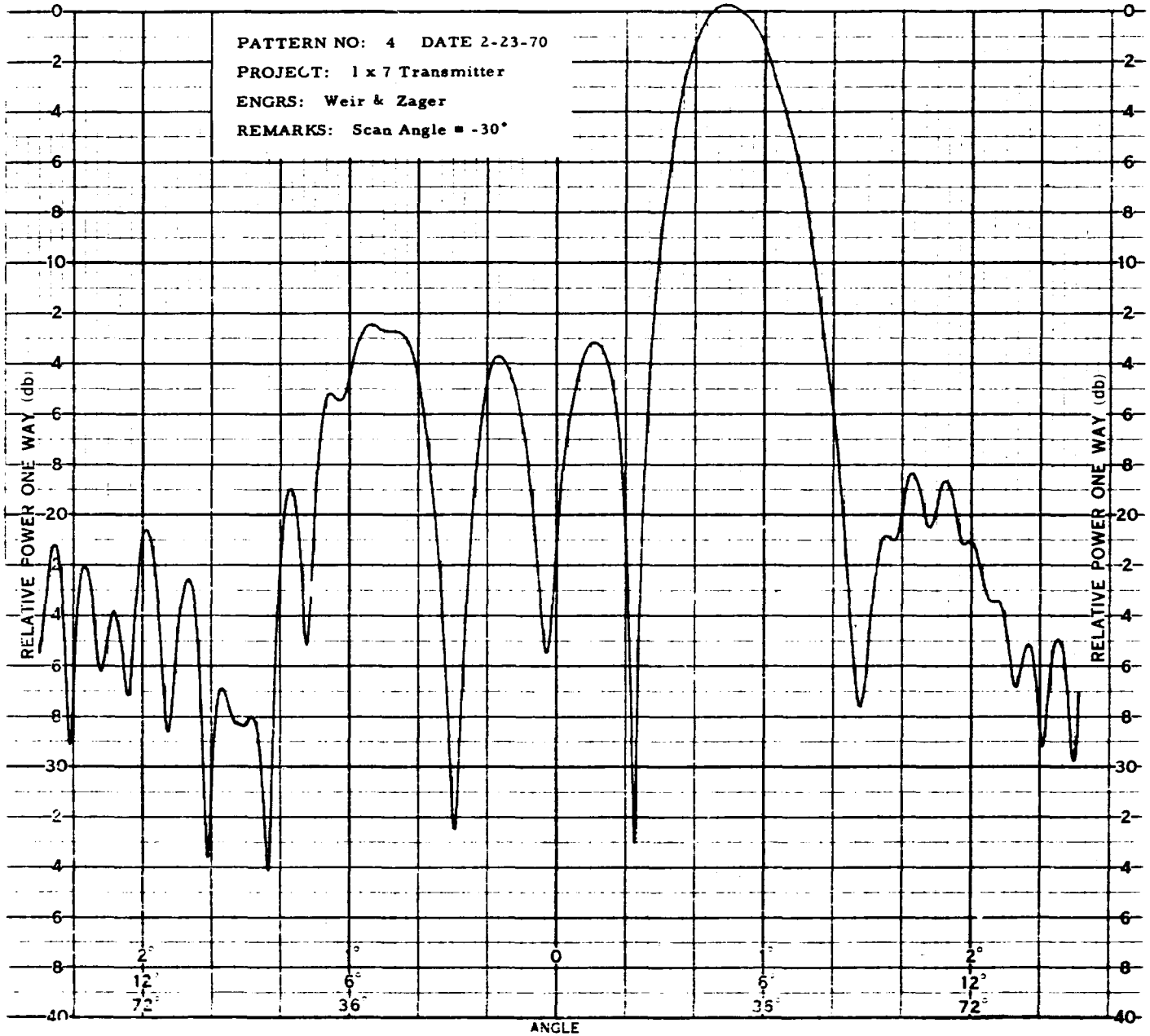
PATTERN NO: 4 DATE 2-23-70
PROJECT: 1 x 7 Transmitter
ENGRS: Weir & Zager
REMARKS: Scan Angle = -30°
RELATIVE POWER ONE WAY (db)
RELATIVE POWER ONE WAY (db)
0
2
4
6
8
10
20
30
40
2°
12°
72°
6°
36°
0
6°
36°
2°
12°
72°
ANGLE

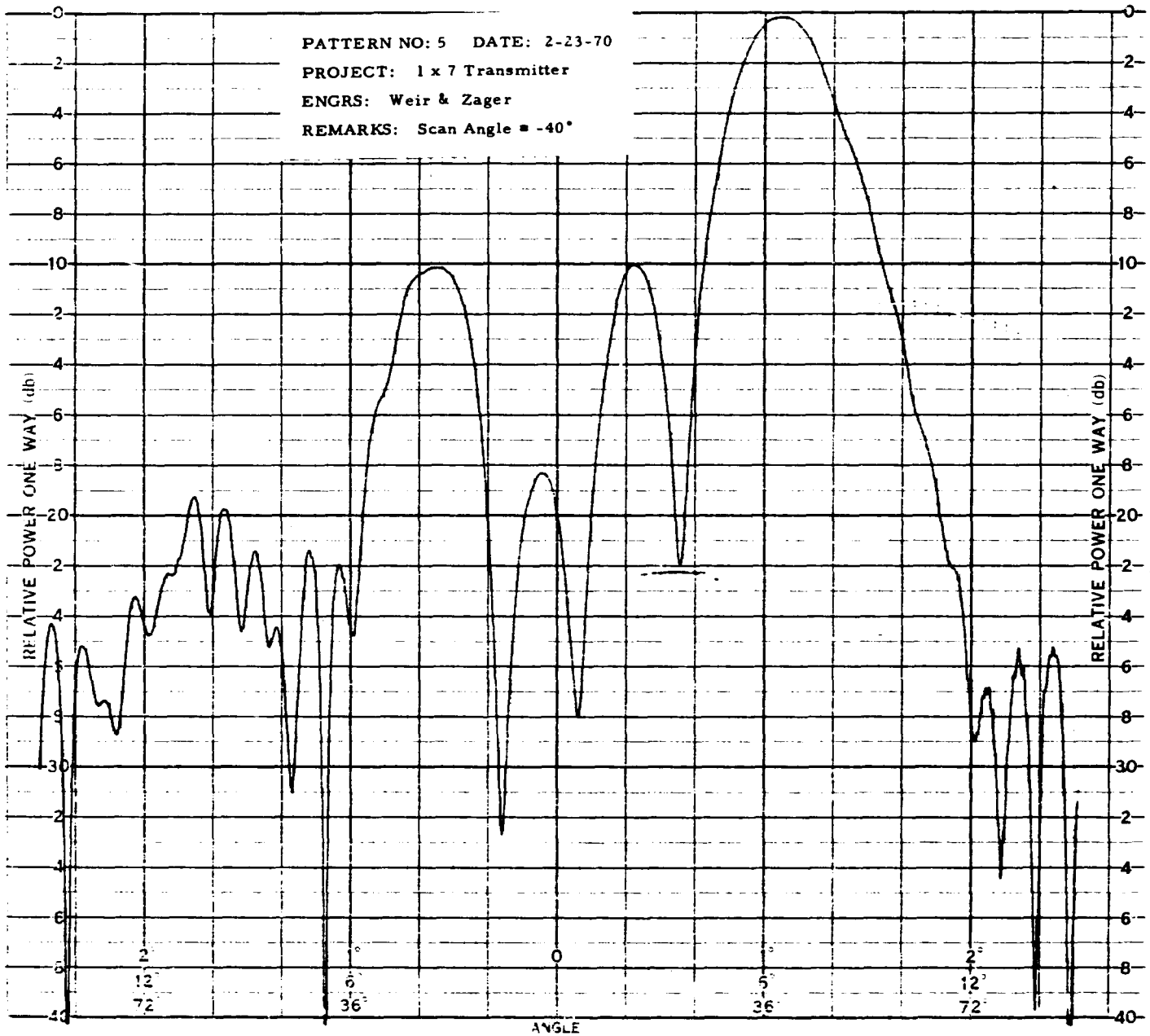
PATTERN NO: 5 DATE: 2-23-70
PROJECT: 1 x 7 Transmitter
ENGRS: Weir & Zager
REMARKS: Scan Angle = -40°
RELATIVE POWER ONE WAY (db)
RELATIVE POWER ONE WAY (db)
0
2
4
6
8
10
20
30
40
2°
12'
72'
1°
6'
36'
0
1°
5'
36'
2°
12'
72'
ANGLE

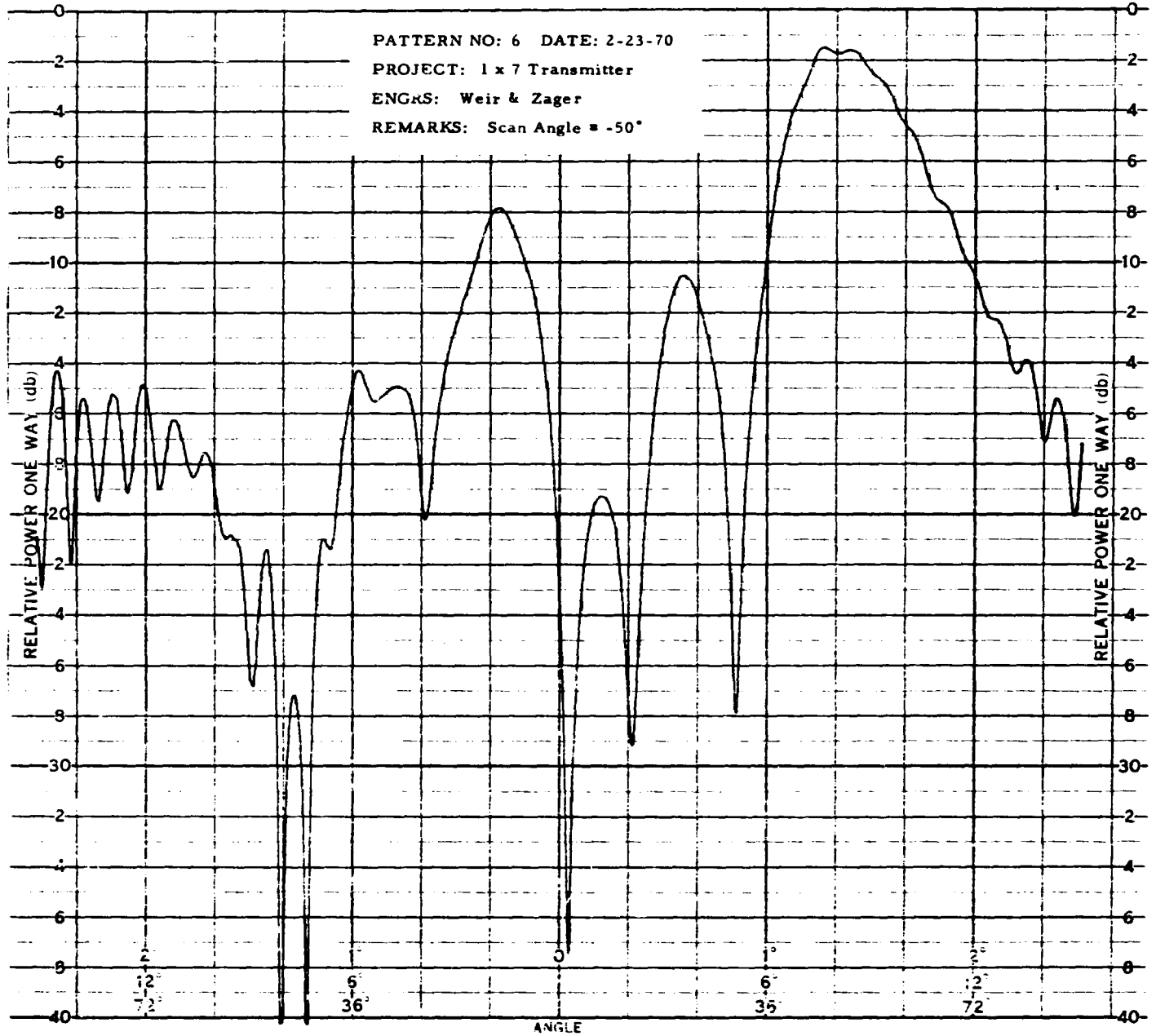
PATTERN NO: 6 DATE: 2-23-70
PROJECT: 1 x 7 Transmitter
ENGRS: Weir & Zager
REMARKS: Scan Angle = -50°
RELATIVE POWER ONE WAY (db)
RELATIVE POWER ONE WAY (db)
0
2
4
6
8
10
20
30
40
ANGLE

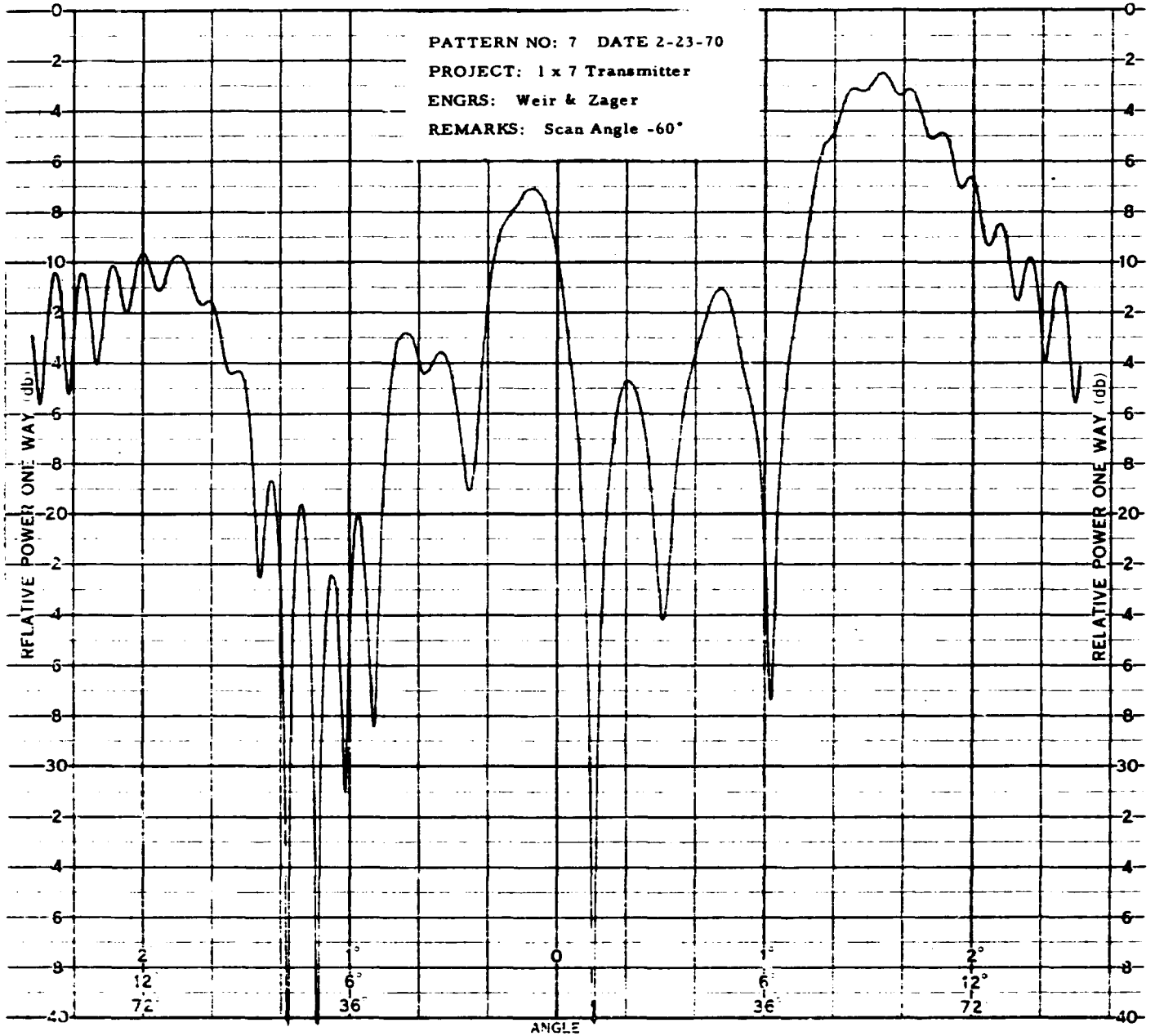
PATTERN NO: 7 DATE 2-23-70
PROJECT: 1 x 7 Transmitter
ENGRS: Weir & Zager
REMARKS: Scan Angle -60°
RELATIVE POWER ONE WAY (db)
RELATIVE POWER ONE WAY (db)
0
2
4
6
8
10
20
30
40
2°
12
72
1°
6°
36
0
1°
6
36
2°
12°
72
ANGLE

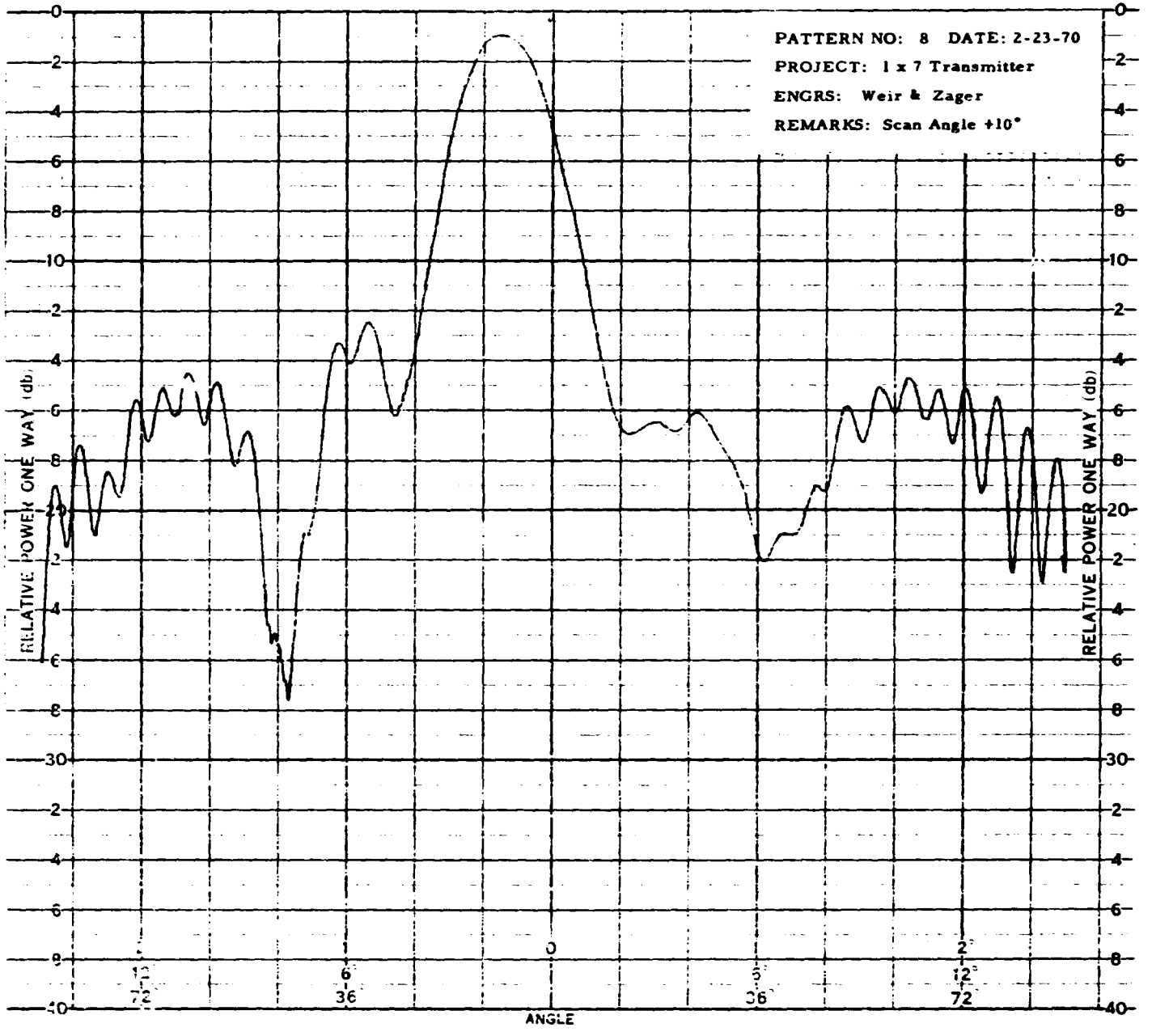
PATTERN NO: 8 DATE: 2-23-70
PROJECT: 1 x 7 Transmitter
ENGRS: Weir & Zager
REMARKS: Scan Angle +10°
RELATIVE POWER ONE WAY (db)
RELATIVE POWER ONE WAY (db)
0
2
4
6
8
10
20
30
40
12
72
6
36
0
3
36
12
72
ANGLE

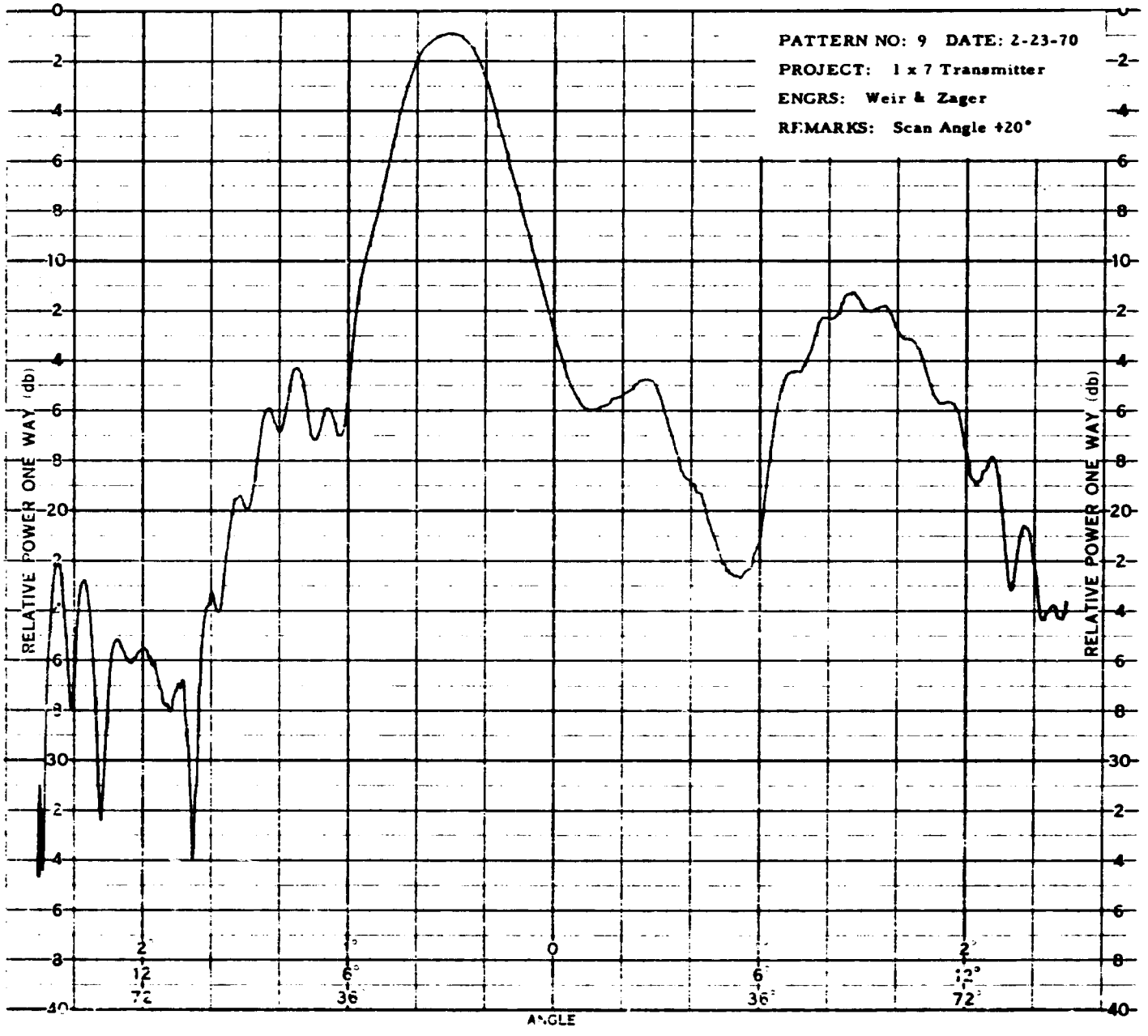
PATTERN NO: 9 DATE: 2-23-70
PROJECT: 1 x 7 Transmitter
ENGRS: Weir & Zager
REMARKS: Scan Angle +20°
RELATIVE POWER ONE WAY (db)
RELATIVE POWER ONE WAY (db)
0
2
4
6
8
10
20
30
40
12°
72
6°
36
0
6°
36
12°
72
ANGLE

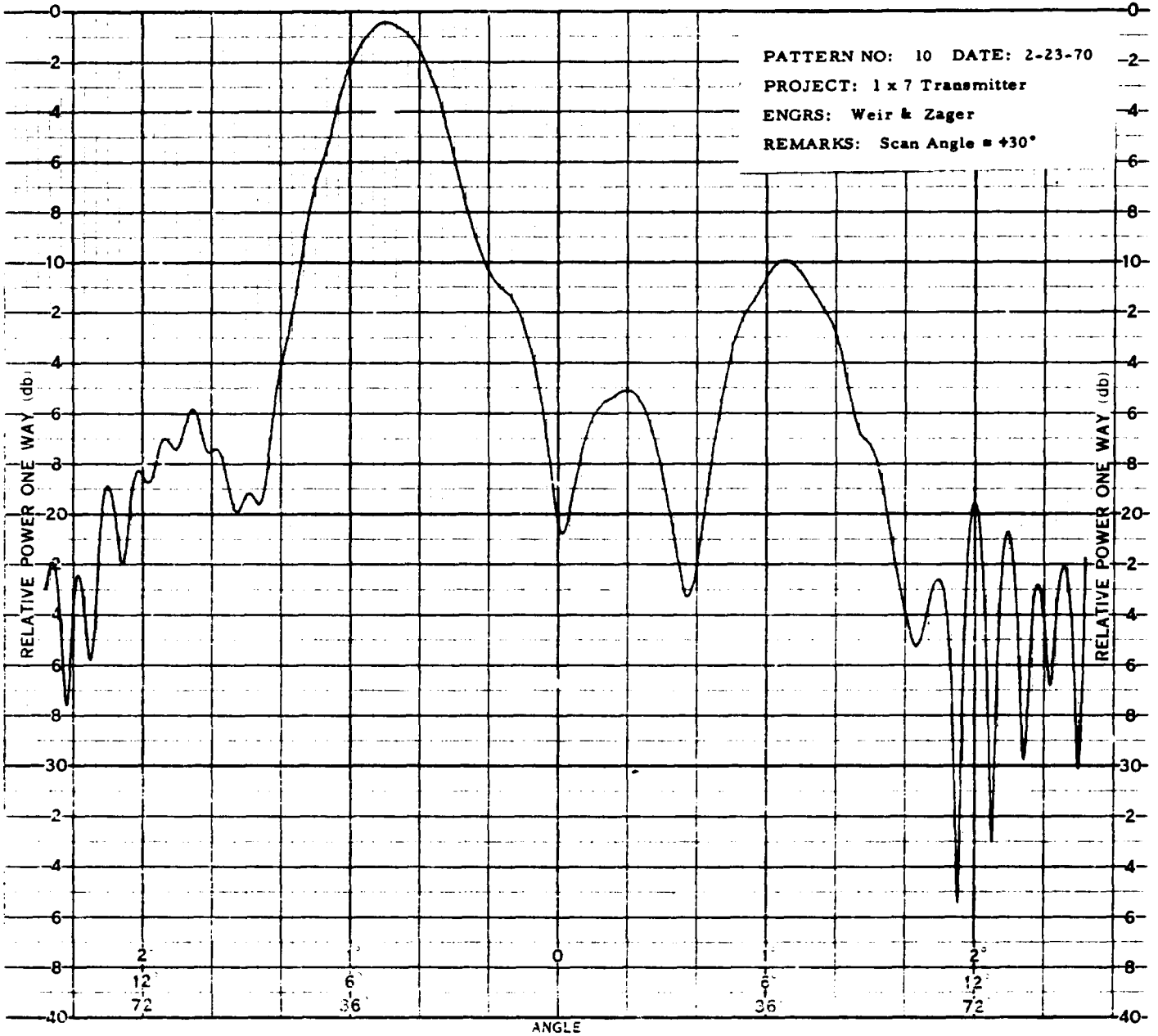
PATTERN NO: 10 DATE: 2-23-70
PROJECT: 1 x 7 Transmitter
ENGRS: Weir & Zager
REMARKS: Scan Angle = +30°
RELATIVE POWER ONE WAY (db)
RELATIVE POWER ONE WAY (db)
0
2
4
6
8
10
20
30
40
2°
12'
72
1°
6'
36
0
1°
6'
36
2°
12'
72
ANGLE

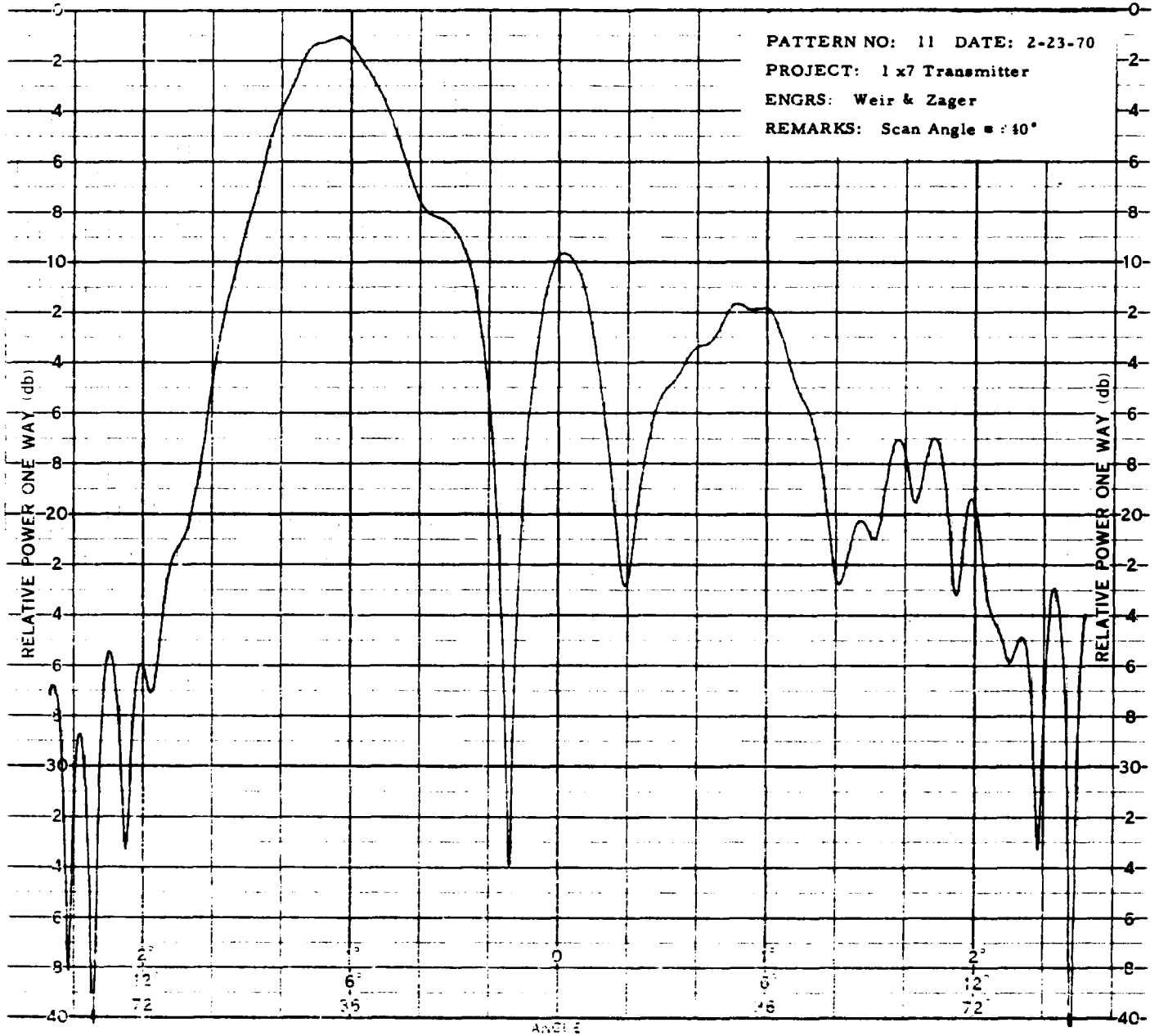
PATTERN NO: 11 DATE: 2-23-70
PROJECT: 1 x7 Transmitter
ENGRS: Weir & Zager
REMARKS: Scan Angle = ±40°
RELATIVE POWER ONE WAY (db)
RELATIVE POWER ONE WAY (db)
0
2
4
6
8
10
20
30
40
12°
72
6°
35
0
6°
36
12°
72
ANGLE

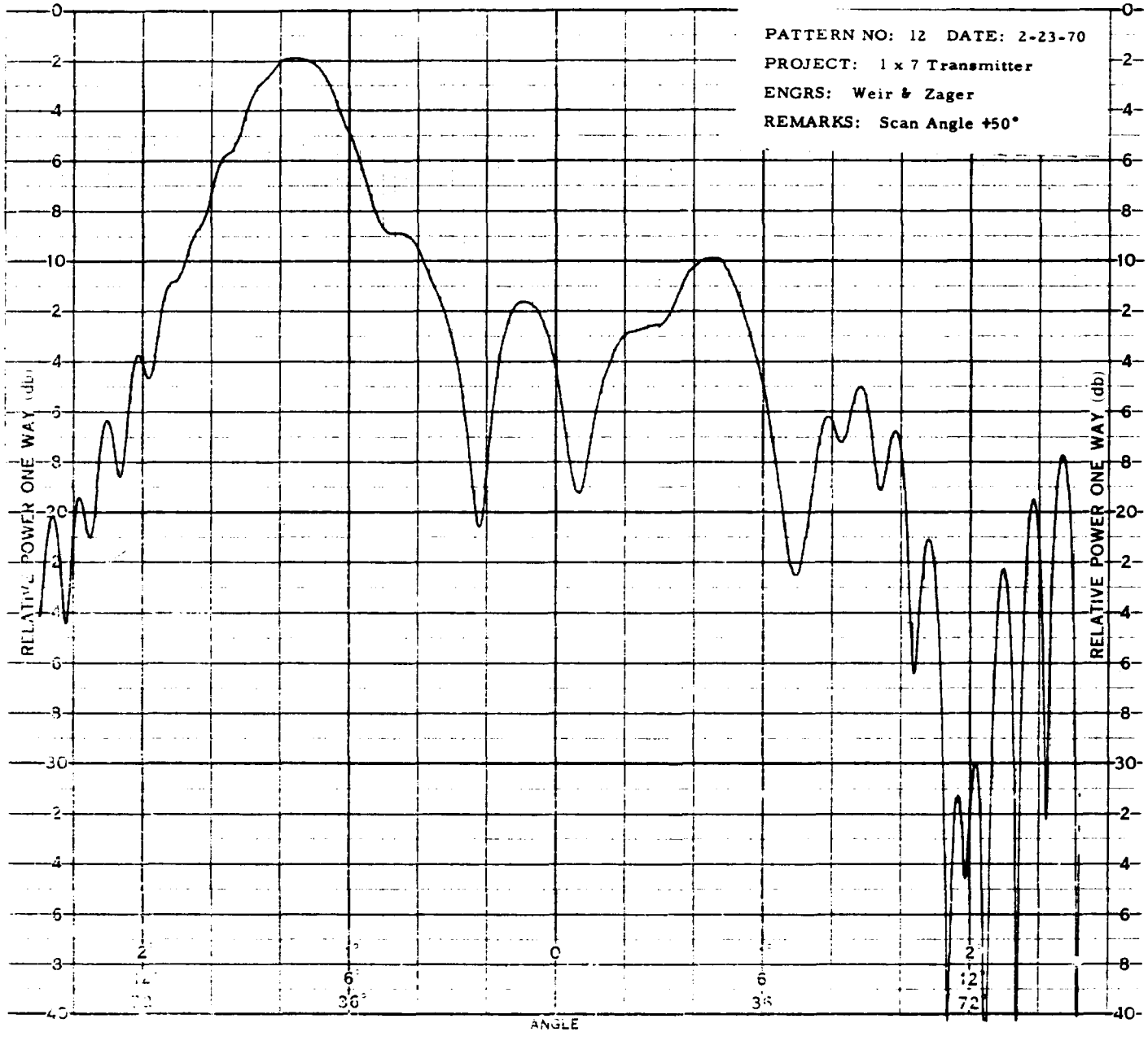
PATTERN NO: 12 DATE: 2-23-70
PROJECT: 1 x 7 Transmitter
ENGRS: Weir & Zager
REMARKS: Scan Angle +50°
RELATIVE POWER ONE WAY (db)
RELATIVE POWER ONE WAY (db)
ANGLE

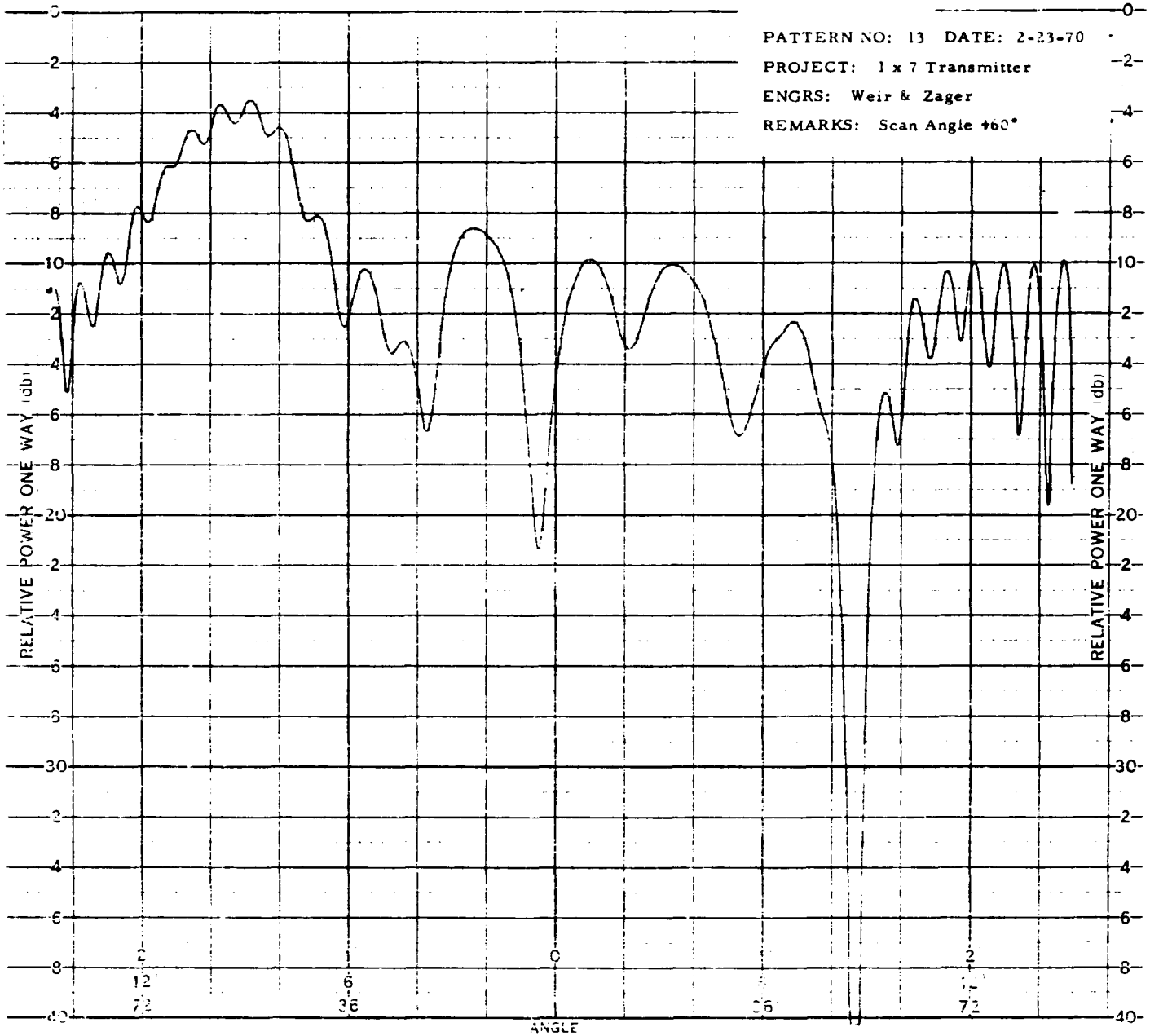
PATTERN NO: 13 DATE: 2-23-70
PROJECT: 1 x 7 Transmitter
ENGRS: Weir & Zager
REMARKS: Scan Angle +60°
RELATIVE POWER ONE WAY (db)
RELATIVE POWER ONE WAY (db)
ANGLE